Revealing losses with impedance spectroscopy in electrochemical energy conversion

Lucas van Elderen

Bachelor Thesis

Physics supervisor: Dr.ir. David A. Vermaas
Mathematics supervisor: Dr. N.V. Budko

Delft Technical University
Applied Sciences

December 8, 2024

Contents

1 Abstract

In this study, a model is developed in COMSOL to investigate the nature of energy losses in ion exchange membranes used in electrochemical energy conversion. By use of electrochemical impedance spectroscopy, the nature of resistance and reactance, and therefore the nature of Ohmic resistances and charge transfer resistances, are evaluated. This is done by first obtaining a model of the setup and the resulting impedance spectrum and then making adjustments in the model to observe the impact on the impedance spectrum as well as the resulting ion concentration profiles. In the used system, the diffusion effects were dominant compared to the double layer effects. Therefore, the impedance spectrum is mainly shaped by the diffusion boundary layer, especially at low frequencies. The ion concentration, diffusion coefficients, and membrane properties were found to have a significant influence on the impedance spectrum. Insights from this study can be used in the optimization of ion exchange membranes and the efficiency of energy conversion systems.

2 Introduction

One of the largest challenges in the field of energy storage and conversion lies in the energy losses inside batteries and fuel cells. Much is still unknown about the origin of chemical energy loss in an ion exchange membrane. To map the source of these losses, electrochemical impedance spectroscopy can be used. This method provides an insight into resistance and reactance mechanisms.
In order to give insight into the exact phenomena inside the electrochemical system that shape the impedance spectrum, an ion exchange membrane can be modeled and its impedance spectrum can be calculated. The model can then be adjusted to measure how these changes affect the impedance, alongside the resulting ion concentrations. This will give a good insight into the exact ion transport that causes the shape of the impedance spectrum, and therefore it will give insight into the nature of the energy losses inside the electrical membrane.

The following research questions will be addressed in this study:

What are the specific ion transport mechanisms within an ion exchange membrane that contribute to the shape of the impedance spectrum?

How do variations in ion concentration and membrane properties influence the impedance spectrum of an ion exchange membrane?

3 Literature Review

Electrochemical conversion technologies

Large-scale conversion of electricity into chemical bonds is one of the largest challenges in green engineering. Electrochemical technologies, such as water electrolysis (for making green hydrogen), CO2 electrolysis (making hydrocarbon chemicals), or electrodialysis (for clean water production), can use the electrical energy to create valuable products. However, despite many developments in the past decades, the energy efficiency still needs to improve further to become competitive with traditional fuel sources.

Hydrogen Production

Hydrogen is one of the most promising energy sources of the future. It has a high energy density, and when burned, the only product is water. Different methods of producing hydrogen are shown in figure 1. A clean and relatively efficient way of producing hydrogen is the use of electrolysis. However, compared to other methods like fossil fuels, the costs are still very high due to high energy consumption (Shiva Kumar, S., Himabindu, V. (2019)).

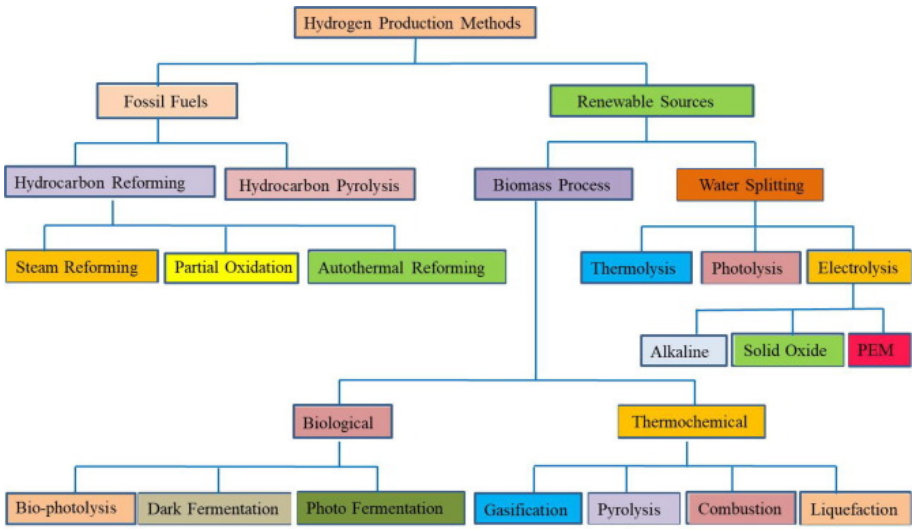

Figure 1: Hydrogen production methods: A schematic of the different hydrogen production methods is shown in the figure. One of the most efficient renewable methods is electrolysis, which is relevant for this research (Kumar & Himabindu, 2019).

Water Electrolysis

Hydrogen can, among other methods, be produced by splitting water using electrochemical water electrolysis. When using clean energy sources like solar or wind in the production of hydrogen, the process has no emissions, and the product is very pure. There are four different methods of hydrogen production using water electrolysis: Alkaline Water Electrolyzer (AWE), Proton Exchange Membrane Water Electrolysis (PEMWE) (or Polymer Electrolyte Membrane Water Electrolyzer (PEME)), Solid Oxide Electrolyzer Cell (SOEC) and Photoelectrochemical Water Splitting (PEC) (Zhang et al., 2020). The basic reaction describing water electrolysis is shown in equation 1. In this research Proton Exchange Membrane Water Electrolysis will be investigated further.

$$2H_2O + Electricity \longleftrightarrow 2H_2 + O_2 \tag{1}$$

Proton Exchange Membrane Water Electrolysis

Proton Exchange Membrane Water Electrolysis (PEMWE) is one of the four main methods of hydrogen production by water electrolysis. It consists of an anode and cathode and a membrane that only conducts protons. PEMWE is the most used method for the production of hydrogen because of the high efficiency and small footprint, among other factors (Kumar & Himabindu, (2019), p446). A schematic of the process and the electrochemical reactions involved are shown in Figure 2.

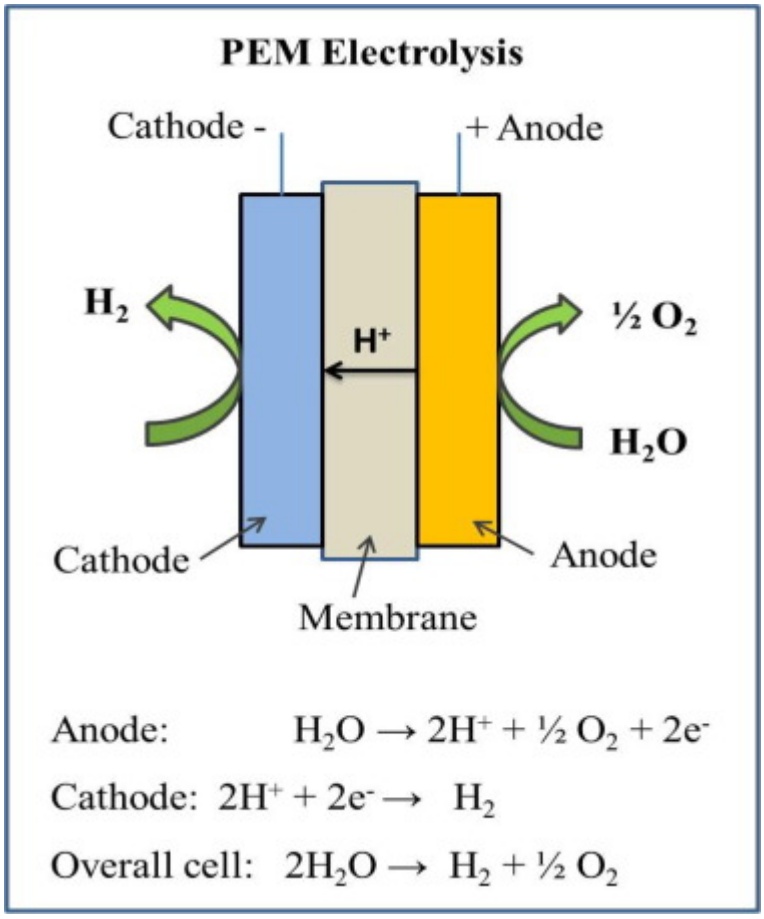

Figure 2: A schematic showing the process of Proton Exchange Membrane water electrolysis and the involved chemical reactions (Kumar & Himabindu, 2019).

CO2 Electrolysis

The reduction of CO_2 emissions is one of the greatest challenges in solving climate change. One way of reducing CO_2 emissions is by using CO_2 in combination with hydrogen to produce useful hydrocarbons. This process is known as CO_2 electrolysis, and the reactions will have the following form (Lin, Zhang, Xu, & Chen, (2023)):

$$xCO_2 + nH^+ + ne^- = C_xH_{n-2y}O_{2x-y} + yH_2O \tag{2}$$

The general process of CO_2 electrolysis always involves ion exchange membranes in one form or another. The five different used methods are shown in figure 3 (Lin, Zhang, Xu, & Chen, (2023), p8).

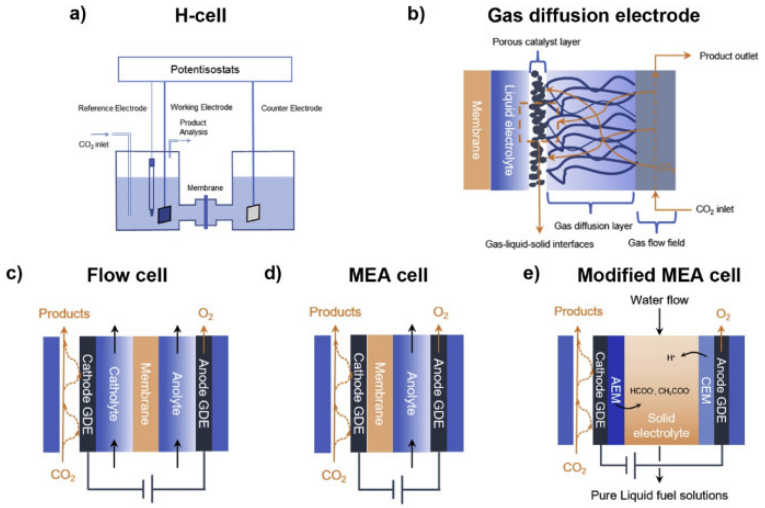

Figure 3

Electrodialysis

Electrodialysis is a process that uses membranes to transport ions in a solution and is mainly used for the desalination of water. Like CO_2 electrolysis and water electrolysis, the method makes use of (ion exchange) membranes. It is a promising technology that can play an important part in solving the issue of a lack of clean drinking water. By using an electric potential, the cations migrate towards the cathode and the anions towards the anode. Because the ion exchange membranes are placed in an alternating sequence, and the cations cannot pass through anion exchange membranes and vice versa, the total flow of cations and anions is restricted. A limiting factor of the efficiency of electrodialysis is the maximum current density. This maximum current density is determined by the ion depletion at the solution-membrane interface (Ahuja, 2014), which will be discussed further.

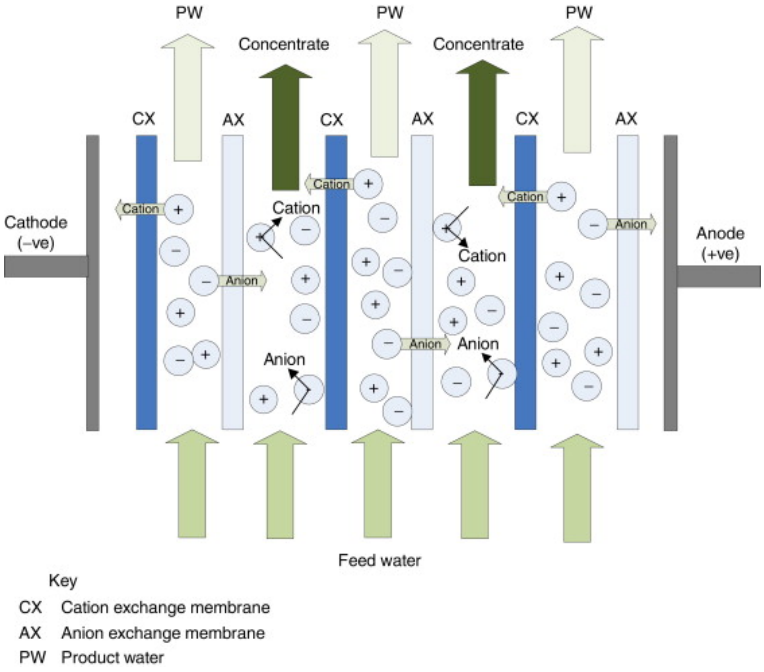

Figure 4: A schematic of an electrodialysis setup. (Ahuja, 2014)

Ion Exchange Membrane

All three electrochemical conversion technologies discussed above make use of ion exchange membranes in one form or another. This research will therefore focus on these membranes and the involved processes that determine their efficiency. There are many different kinds of ion exchange membranes from which the most known are the cation exchange membrane (CEM) and the anion exchange membrane (AEM). Like the name suggests, the CEM only permits cations (positive ions), and the AEM only permits anions (negative ions). For our research we will focus on the CEM, although many of the results will be similar to those for an AEM.

The cation exchange membrane contains fixed negative ions and can only permit cations, while the opposite is true for the anion exchange membrane. This is illustrated in figure 5 [**Astom**].

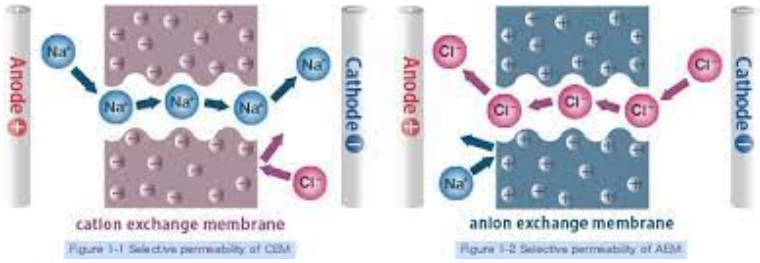

Figure 5: A schematic view of cation and anion exchange membranes.

Electrochemical Impedance Spectroscopy

A way to measure energy losses inside electrochemical energy conversion is Electrochemical Impedance Spectroscopy (EIS). This method measures the impedance of a system for different frequencies of AC voltage. The impedance is effectively the resistance of an electric system to an alternating current. By measuring the impedance for different AC frequencies, a spectrum can be obtained. The shape of this spectrum then gives us information about the cause of impedance and therefore the cause and location of energy losses.
In electrochemical impedance spectroscopy, the impedance is effectively calculated from the electric potential and the measured current (or the current and measured potential). This relation is given by:

$$Z = \frac{dV}{dI} \tag{3}$$

Which for resistances simplifies to equation 4:

$$Z = \frac{V}{I} \tag{4}$$

Where V is the potential, I the current, and Z the impedance. This impedance Z has two components, one real and one imaginary. The real part is known as the resistance R, and the imaginary part is the reactance X, such that Z can be written as:

$$Z = R + jX \tag{5}$$

This reactance in an electrochemical cell can be caused by some sort of a capacitor and is measured in the form of a phase shift, or delay, in the measured current, while resistance causes a scaling in the amplitude of the measured current. Different physical processes can act like capacitors, which will be explained later. In an

electrochemical impedance spectrum, the resistance is plotted on the x-axis and the reactance on the y-axis. For every AC frequency, one data point can then be calculated. For many different frequencies, an impedance spectrum can then be created.

Measuring Resistance

The resistance of the setup can be caused by multiple different phenomena. The first one is the resistance of the ion exchange membrane. This is a constant resistance that is not dependent on the concentration of the species. The second resistance is caused by the double layer. Because the membrane has a fixed charge, this attracts a layer of opposite charge that forms a double layer at the surface of the membrane. This double layer 'blocks' the current and in that way forms a resistance. The last component of the resistance is caused by the diffusion boundary layer. Since the ion exchange membrane only lets through one of the two species, there will be a buildup of the species at the boundaries of the membrane. This difference in concentrations is called the diffusion boundary layer.
The three resistances R_M, R_{DL} and R_{DBL} all have different contributions at different frequencies of the alternating current. At very high frequencies the membrane resistance will be dominant because the double layer and boundary layer won't have time to build up. At very low frequencies the diffusion boundary layer will be dominant because the size of this layer is much larger than the double layer (μm vs nm scale).
Finally we have the solution resistance R_S. This resistance depends on the temperature, type of ions, ion concentration, and geometry of the cell.

Reactance of the cell

The reactance of the cell is the amount of phase shift of the measured current (Bardini, 2020). The reactance is therefore a result of capacitor-like effects inside the cell. There are two possible reasons for the cell to behave like a capacitor: the electrical double layer (DL) and the diffusion boundary layer (DBL).

Electric Double Layer

Because the membrane has a certain fixed charge, the membrane will attract ions with opposite charge. These ions will stick to the membrane surface and will form a layer of charge (Długołęcki et al., 2010). This layer can be charged and uncharged depending on the potential.

Diffusion Boundary Layer

The diffusion boundary layer of the membrane is the region of the electrolyte where the concentrations of the ions are different from the bulk solution. Like the name suggests, this layer is formed by the diffusion of the ions, which grows after some time. Therefore, the effect of this diffusion boundary layer will be the greatest at low frequencies. The diffusion boundary layer 'stores' charge and can discharge again when it disappears. In this way the layer works like a capacitor. The diffusion boundary layer, however, is far from a perfect capacitor. Usually the DBL is therefore modeled as a constant phase element Q (Długołęcki et al., 2010). This constant phase element represents a non-ideal capacitor, which shows in impedance spectra as depressed semicircles. This non-ideality can be expressed by n, which lies between 0 and 1, where an n of 1 represents an ideal capacitor.
These different processes are shown in figure 6. The diffusion boundary layer exists at low frequencies, while the double layer forms at medium frequencies. The electric double layer still exists at very high frequencies, but its effects are overshadowed by other phenomena like Warburg impedance. Although these frequencies differ for different solutions and membranes, the low-frequency domain ranges usually from one to a few hundred Hertz, while the medium frequencies entail values up to a few kHz. Because of electroneutrality, electric double layers cannot be modeled. The used frequency range will therefore be 0.001 to 10 kHz.

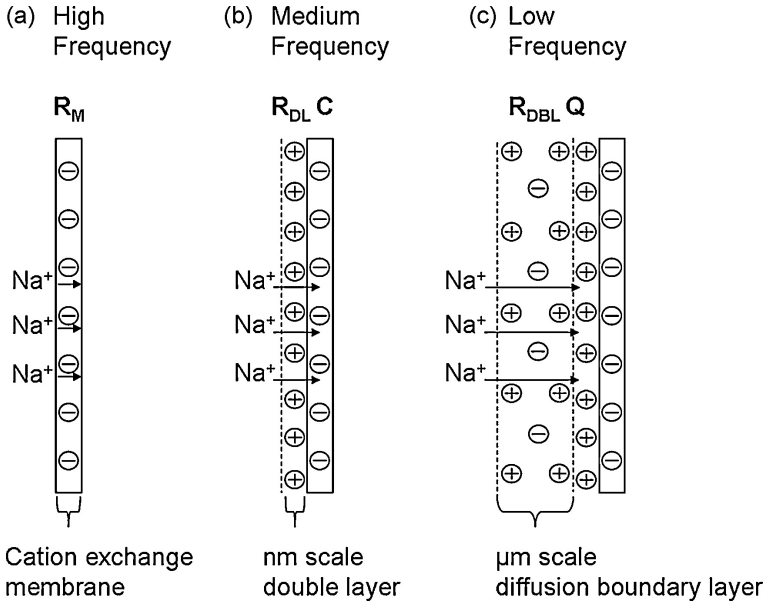

Figure 6: Different phenomena occur for varying frequencies. (Długołęcki et al., 2010)

Impedance of an ion exchange membrane

Two examples of experimentally obtained impedance spectra for ion exchange membranes are described in (Długołęcki et al., 2010b) and in (Zhang et al., 2016). In both of the studies, the impedance measurements were fitted to the same theoretical electric system. This electric system is characterized by an equivalent circuit shown in figure 7:

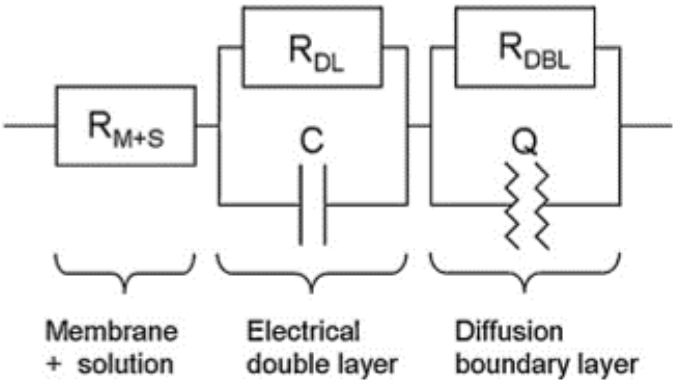

Figure 7: Equivalent circuit for an ion exchange membrane with electrolytes. (Długołęcki et al., 2010)

Here R_{M+S} is the combined membrane and solution resistance, R_{DL} and R_{DBL} are the double layer and diffusion boundary layer resistances, C is the double layer capacitance, and Q is the constant phase element that describes the capacitance of the diffusion boundary layer.
The equivalent circuit is in both studies fitted to the experimental impedance data, which yields the following fits:

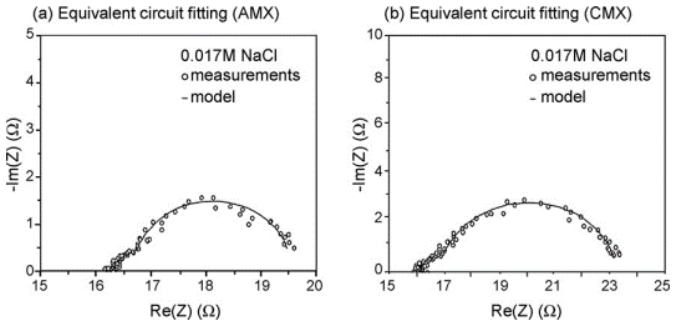

Figure 8: The equivalent circuit fitted to the measured impedance for an anion exchange membrane and a cation exchange membrane. (Długołęcki et al., 2010)

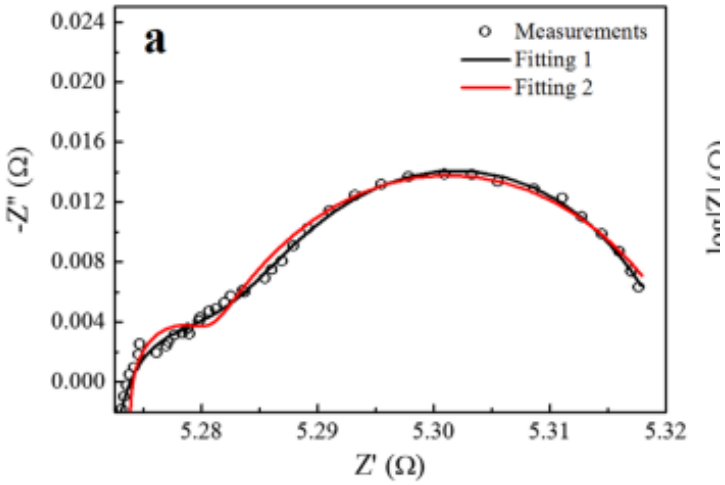

Figure 9: The equivalent circuit fitted to the measured impedance of a cation exchange membrane. The first fit assumes the same equivalent circuit as described in figure 7 while the second fit also assumes the double layer to be a constant phase element. (Zhang et al., 2016)

The large semicircle on the right is formed by low frequencies between 0.01 Hz and 1 Hz for the second study and by frequencies between 0.001 Hz and 0.1 Hz in the first study, while the quasi-linear impedance is formed by medium to high frequencies ranging from 1 Hz to 1 kHz. This implies that in both studies the impedance spectrum is for the largest part determined by the diffusion boundary layer, which is most defined at lower frequencies.
The studies, however, are based on measured data with parameters that cannot be easily varied. In this research the measurement error is much smaller, and relevant parameters can easily be investigated.

Finite Element Method

In order to model the physical problem, several partial differential equations need to be solved. Generally, these equations cannot be solved analytically. Therefore, COMSOL approximates the solution using numerical discretizations. The technique that is used to do this is called the Finite Element Method (FEM) (Zienkiewicz, O. C., & Taylor, R. L. (2000)).
The Finite Element Method breaks down the domain into finite elements, at which local solutions are approximated. The main steps in FEM are the discretization of the domain, the formulation of the weak form of the PDEs, and creating the system of equations (Detailed Explanation of the Finite Element Method (FEM), n.d.-b).

In this study, FEM is applied to solve the Nernst-Planck equations and the Poisson equation, using quadratic basis functions for improved accuracy.

Time-Integration Method

The used solver type is implicit, and the method is the Backward Differentiation Formula (BDF). The Backward Differentiation Formula is often used for solving stiff systems, such as the coupled PDEs in this model, due to its implicit formulation and stability properties. The minimum BDF order is 1 (which is equivalent to the backward Euler method), and the maximum order is 2. This means that COMSOL switches between order 1 and 2 based on the behavior of the solution. The Backward Differentiation Formula is shown in equations 6 and 7 for orders 1 and 2, respectively.

$$u_{i+1} = u_i + hf(u_{i+1}) \tag{6}$$

$$3u_{i+1} = 4u_i - u_{i-1} + 2hf(u_{i+1}) \tag{7}$$

Where u is the vector or variable that is calculated, h is the step size, and f is a non-linear function.

Newton-Raphson Method

The used solver is Newton's method (or Newton-Raphson), which is non-linear. The Newton-Raphson method is chosen because it is stable and efficient in solving the nonlinear system (Frei, 2020). The general idea of the Newton-Raphson method is to solve equation 8 (Vuik et al., 2023):

$$u = hf(u) + v \tag{8}$$

Where u is the vector or variable that is calculated, h is the step size, f is a non-linear function, and v is a known vector that represents the boundary conditions. In order to calculate u, $u - u_i$ is approximated by equation 9.

$$u - u_i \approx p_i(u_i) \tag{9}$$

The initial value u_i is known, and $p_i(u_i)$ is the correction term associated with u_i. Then u_{i+1} is given by equation 10.

$$u_{i+1} = u_i + p_i(u_i) \tag{10}$$

The correction term in the Newton-Raphson method is given by equation 11.

$$p_i(u_i) = -\frac{f(u_i)}{f'(u_i)} \tag{11}$$

Richardson Extrapolation

To test the numerical accuracy of the model and the necessary mesh size and time step, the Richardson extrapolation method is used. Richardson extrapolation uses different mesh sizes or time steps to approximate the true value of a certain parameter, such as ion concentration or potential. In this way the associated error for different meshes can be obtained and the numerical accuracy can be evaluated. The method is suitable to address discretization errors but is sensitive to higher-order errors and solver tolerances (Embree, M. (2006)).

4 Methodology

Materials and Methods

For the modeling of the membrane and electrolyte, multi-physics simulation software COMSOL is used. Advantages of using this software instead of a real-life setup are the lack of noise and measurement errors. Moreover, many different setups can be tested this way. For the model, the tertiary current distribution with a Poisson charge conservation model in COMSOL is used. This module works with a predetermined set of equations to calculate the concentrations of the species at different times in the whole domain.
First the membrane and electrolytes are created. The membrane contains a fixed space charge, ρ, which can be varied and which is negative. For a negatively charged membrane, cations will be able to pass, while anions are blocked. Therefore, the membrane is a cation exchange membrane. Three different species are used for the model: A, B, and C, from which A are cations and B and C are anions. The fixed space charge is defined in the model but is not caused by one of the species. By choosing two anions, the effectiveness of the membrane can also be investigated. This is one of the main goals of the COMSOL blog that is used as a basis for the model (Ekström, 2021), but it is less relevant for the investigation of the impedance. Therefore a model with only one anion would also be sufficient for this study. To avoid discontinuities in electric potential and their corresponding concentration discontinuities, boundary regions are defined at the membrane boundary in which the mesh is more detailed. The size of the electrolytes L_{El} and of the membrane L_{Mem} can be varied. For simplicity, the model is one-dimensional. For measuring the impedance, a harmonic potential perturbation is introduced to the electrolyte, after which the current is measured. These voltage and current signals can then be translated to an impedance measurement. For different frequencies, different impedance measurements can be conducted to form an impedance spectrum. Other parameters that can be adjusted are the domain size (of the membrane and electrolytes), the species concentration, the temperature, the diffusion coefficients of the species, the fixed space charge of the membrane, and the perturbation amplitude.

Ion Concentration Profiles

For every measurement, the concentration profile during the whole measurement window is recorded in order to map the transport of ions for different impedances. This way, a better relationship between the impedance and the actual ion transport can be determined. From these concentration profiles, the diffusion boundary layer

and the electric double layer can, for example, be identified.

Model Specifications

A schematic setup of the model in COMSOL is shown in figure 10. The used model is largely based on the model described at the official COMSOL website about ion-exchange membranes and Donnan potentials (Ekström, 2021).

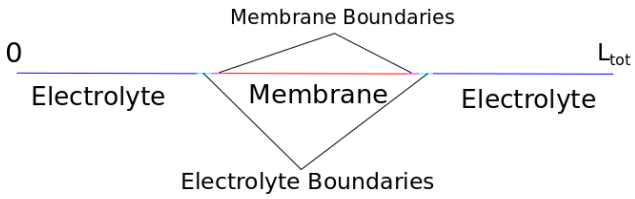

Figure 10: A schematic view of the setup in COMSOL is shown. The membrane is surrounded by electrolytes and is divided into three regions: a central large domain and two smaller boundary domains to capture steep gradients. Similarly, the model includes four electrolyte domains: two larger bulk domains and two smaller boundary domains, also designed to capture steep concentration and potential gradients.

Boundary conditions and equations

In order to be able to obtain a solution, COMSOL needs certain input in the form of boundary conditions. The bulk concentrations of all of the ions need to be constant at the boundaries and are defined by the following equations.

$$A(x = 0) = A_0 \tag{12}$$

$$B(x = 0) = B_0 \tag{13}$$

$$C(x = 0) = 0 \tag{14}$$

$$A(x = L_{Tot}) = A_0 \tag{15}$$

$$B(x = L_{Tot}) = 0 \tag{16}$$

$$C(x = L_{Tot}) = C_0 \tag{17}$$

The most important equation in COMSOL is the Nernst-Planck equation, which describes the transport of the ions:

$$\frac{\partial c_i}{\partial t} + \nabla \cdot J_i + u \cdot \nabla c_i = R_i \tag{18}$$

Where c_i is the concentration of species i, J_i is the flux of species i, u is the velocity field, and R_i is a source of species i. The velocity field can be defined in the electrolyte and the membrane and is set to 0 for simplicity.
The flux is defined in COMSOL by equation 19:

$$J_i = -D_i \nabla c_i - z_i u_{m,i} F c_i \nabla \phi_l \tag{19}$$

Where D_i denotes the diffusion coefficient of species i, $u_{m,i}$ is the mobility of species i, and ϕ_l is the electric potential.
The chosen charge conservation model is Poisson, which relates the electric potential to the charge density:
The Poisson equation is as follows:

$$\nabla \cdot (-\epsilon \nabla \phi_l) = \rho \tag{20}$$

With ϕ_l the electric potential of the electrolyte, ϵ is the permittivity, and ρ is the space charge density. The relative permittivity is taken to be equal to one, so the permittivity is equal to the permittivity of free space ϵ_0, but can later be varied to resemble a realistic system.
The space charge density contains two components, the fixed space charge and the mobile ions. Therefore, in the ion exchange membrane, the space charge density is as follows:

$$\rho = F \sum_{i}^{3} z_i c_i + \rho_{fix} \tag{21}$$

Where F is Faraday's constant, z_i is the charge of ion i, c_i is the concentration of ion i, and ρ_{fix} is the fixed space charge density. Because the fixed space charge is zero outside of the membrane, the space charge in the electrolytes is equal to:

$$\rho = F \sum_{i}^{3} z_i c_i \tag{22}$$

Model Building

When the relevant equations are defined, the geometry can be constructed. Seven domains are created; the first and last domain will have a length of 4L, where L is equal to $50\mu m$ but which can be varied. The second and sixth and the third and fifth domains have length L/1000, and the fourth domain has length L. These extra small domains are defined to avoid discontinuities in concentrations and be able to model electric double layers. The mesh size in these domains will be set to be extremely small. The electrolyte consists of domains 1, 2, 6, and 7, while the membrane consists of domains 3, 4, and 5.
The Tertiary Current Distribution with Nernst-Planck-Poisson charge conservation now needs some basic settings. First, the species charge is set to 1 for species A and to -1 for species B and C. The temperature is set to be equal to the default temperature.

Electrolyte

In COMSOL the Poisson equation is transformed into a different form. The electric displacement field D_l is defined by equation 23:

$$D_l = -\epsilon_0 \epsilon_r \nabla \phi_l \tag{23}$$

Where ϵ_0 is the permittivity of free space and ϵ_r is the relative permittivity. The relative permittivity is usually between 20 and 100, and the default value is taken to be 50. Combining Gauss's law

$$\nabla \cdot D_l = \rho \tag{24}$$

and equation 22 yields the equation used in COMSOL:

$$\nabla \cdot D_l = F \sum_{i}^{3} z_i c_i \tag{25}$$

Now the electrolyte needs a convection input. For this research there is no convection, so the velocity field u is set to 0. The diffusion coefficients can then be defined. Usually diffusion coefficients are around 1e-9 m^2/s, so these will be the initial values, but the diffusion coefficients can later be varied. For the migration in the electric

field, the Nernst-Einstein relation is used:

$$u_{m,i} = \frac{D_i}{RT} \tag{26}$$

Where $u_{m,i}$ is the mobility coefficient of ion i, D_i is the diffusion coefficient of ion i, and R and T are the gas constant and the temperature (which is the default temperature of 293.15 K). D_i can be varied to study the effects of different mobilities on the impedance.
Finally the relative permittivity $\epsilon_r$is determined and set to 50 for the electrolyte and 20 for the membrane.
Now the no-flux condition, initial values, and boundary conditions are applied as described earlier. In COMSOL these conditions can be applied by adding no-flux or boundary conditions and initial values in the physics interface.

Ion Exchange Membrane

For the ion exchange membrane, the Nernst-Planck-Poisson equations look slightly different:

$$\frac{\partial \epsilon_l c_i}{\partial t} + \nabla \cdot J_i + u \cdot \nabla c_i = \epsilon_l R_i \tag{27}$$

Where ϵ_l is the electrolyte volume fraction, which determines how porous the membrane is. Dense membranes will have an electrolyte volume fraction close to 0, while for porous membranes the electrolyte volume fraction will be closer to 1. Usually ϵ_l ranges from 0.2 to 0.8 (Sata, 2007), but for this setup it is set to be 0.5. However, the electrolyte volume fraction can be varied to study its effects on the impedance. The ion exchange membrane partly consists of an electrolyte, the space where ions can flow. The electrolyte volume fraction denotes the fraction of the electrolyte volume compared to the total volume:

$$\epsilon_l = \frac{V_{electrolyte}}{V_{Total}} \tag{28}$$

Because the membrane consists of a porous structure compared to the free space of the electrolyte, the ion transport will be impeded. Therefore, COMSOL uses an effective transport parameter correction. For this research, Bruggeman is used, which results in the following equations:
The flux is defined in COMSOL by equation 29:

$$J_i = -D_{i,eff} \nabla c_i - z_i u_{m,i,eff} F c_i \nabla \phi_l \tag{29}$$

The effective diffusion coefficient $D_{i,eff}$ is determined by the Bruggeman correction in equation 30:

$$D_{i,eff} = \epsilon_l 1.5 D_i \tag{30}$$

The electric displacement field is given by equation 23, where ϵ_r is the relative permittivity of the ion exchange membrane, and for the Poisson equation, the fixed space charge term is added:

$$\nabla \cdot D_l = F \sum_{i}^{3} z_i c_i + \rho_{fix} \tag{31}$$

The fixed space charge ρ_{fix} is set to be equal to 0.1 M of a negative ion, which amounts to about -9.65 e6 C/m^3, which can be varied.
The relative permittivity of an ion exchange membrane is usually between 2 and 80. The default value is chosen to be 20 and can be varied.
The convection, diffusion, and migration are set to be equal to those in the electrolyte.

Richardson Extrapolation

The Richardson extrapolation uses different mesh sizes or time steps to evaluate the accuracy of the solver. The error estimate is of particular interest and is given by equation 32:

$$u(x) - v(x, h) = Ch^p \tag{32}$$

Where u(x) is the unknown exact solution at x and v(x, h) is the numerical solution at the same location obtained with the (maximum) element size h. C is the error coefficient that quantifies the magnitude of the leading-order discretization error, and p is the order of convergence. For finer discretizations h, C should decrease.
From the error estimate, p, u, and C can be determined when three different measurements of v are known (with different h). When solving the system of equations: Richardson extrapolation assumes that the error in the approximation decreases polynomially in the discretization parameter, which is the mesh element size or the time step. Now u(x) can be estimated as follows: For two h, the error model is given by:

$$u(x) - v(x, h_1) = Ch_1^p \tag{33}$$

$$u(x) - v(x, h_2) = Ch_2^p \tag{34}$$

More values of h can be used to refine the estimate for p, but only two are necessary for an initial estimate.
Now the equations are subtracted and solved for C:

$$v(x, h_2) - v(x, h_1) = C(h_2^p - h_1^p) \tag{35}$$

$$C = \frac{v(x, h_2) - v(x, h_1)}{h_2^p - h_1^p} \tag{36}$$

Now C is substituted into one of the error equations, which is solved for u(x) to give the Richardson extrapolated result.

$$R(h) = \frac{f_1 h_1^p - f_2 h_2^p}{h_1^p - h_2^p} \tag{37}$$

Where R(h) is the Richardson extrapolated result, f_1 and f_2 are the results obtained using discretization sizes h_1 and h_2 respectively ($v(x, h_1)$ and $v(x, h_2)$) and p is the order of the error. The order of error can be estimated by equation 38:

$$p \approx \frac{\log(\frac{v(h_2)-v(h_1)}{v(h_3)-v(h_2)})}{\log\left(\frac{h_2}{h_3}\right)} \tag{38}$$

Because the current and potential both depend on the ion concentrations, this will be the parameter of interest. The concentration of specie A is measured at the boundary between the first and second domain (at a distance L/1000 left of the membrane) after 0.1 s.

Largest mesh size h (μm)	**Number of elements**	**Concentration cA** (mol/m^3)
18.182	100	9.9599898
9.091	200	9.9598695
4.545	400	9.9598549
2.273	800	9.9598475
1.136	1600	9.9598541
0.568	3200	9.9598554
0.284	6400	9.9598377

Table 1: The concentration of specie A at the interface between the first two domains after 0.1 s for different element sizes.

For two values of h, the Richardson extrapolate can lead to inconsistent results. Therefore, to improve the Richardson estimate, multiple h will be used at the same time. This results in a higher-order extrapolation formula in which the leading error of all h combined is minimized.
This leads to a least-squares Richardson extrapolation that minimizes the error term given by equation 39:

$$\sum_{i=1}^{n} (v(x, h_i) - (u + Ch_i^p))^2 \tag{39}$$

The results of this least-squares minimization are shown in table 2 and are calculated by Python code, which is listed in the appendix.

Number of h values	$R(h)$ **[mol/m^3]**	**Error Coefficient** (C)	**Convergence Order** (p)
3	9.959851	5.27e-08	3.05
4	9.959850	5.23e-08	2.98
5	9.959849	5.14e-08	2.88
6	9.959849	5.09e-08	2.80
7	9.959849	5.07e-08	2.73

Table 2: Results of Richardson extrapolation using subsets of mesh sizes, showing the extrapolated concentration, error coefficient C, and convergence order p.

For all numbers of used h, the numerical solutions are stable since $p > 2$. This means the used FEM formulation is accurate and the solution is converging when the mesh is refined.

Richardson extrapolation can also be used to evaluate the chosen time steps and the resulting error. Again, the concentration of specie A is calculated at the boundary between domain 1 and 2 after 0.1 s for different time steps. A constant mesh consisting of 400 elements is used.

Time step h (s)	**Concentration cA** (mol/m^3)
0.1	9.9598548610
0.05	9.9598548635
0.025	9.9598548644
0.0125	9.9598548557
0.00625	9.9598548498
0.003125	9.9598548504
0.0015625	9.9598548595

Table 3: Time steps, h, and corresponding concentrations.

To improve the Richardson extrapolate, multiple h will be used for the time step as well. These results are shown in table 4:

Number of h	$R(h)$ **[mol/m^3]**	**Error Coefficient (C)**	**Convergence Order (p)**
3	9.959855	6.00e-06	2.69
4	9.959855	-4.80e-05	4.26
5	9.959855	-2.30e-05	3.03
6	9.959855	-5.90e-05	4.16
7	9.959855	2.00e-06	2.20

Table 4: Richardson extrapolation results for increasing subsets of time steps.

For the time steps, the convergence orders are also larger than 2, which indicates a stable numerical solution. Since the solution is converging well, the time steps don't need to be further refined. The large fluctuations in the convergence order and the negative error coefficients could indicate rounding errors at very small time scales or the domination of solver tolerances. This shows the limitations of the Richardson method, although the convergence order remains above 2, which indicates accurate results.

In summary, the extrapolated results for the concentration of specie A at the electrolyte-membrane interface for a 1 Hz potential after 0.1 s is about $9.959855 mol/m^3$ for both the mesh and time steps. The convergence order varies from 2.7 to 3.0 for the mesh and from 2.2 to 4.3 for the time steps. The large variability in the convergence order for the time steps is likely due to numerical limitations at very small steps. The optimal mesh size consists of 400 elements because the concentration is very close to the Richardson extrapolate, and the convergence order is much higher than 2, so the method is already solving the problem accurately. Increasing the number of elements will therefore not significantly improve the results. For different time steps, the solution does not significantly change. In combination with a convergence order larger than 2, a time step of 0.01 s will be sufficient.

Mesh and Discretization of the Domain

The domain is split into seven different components: two in both electrolytes and three in the membrane. The four domains at the electrolyte-membrane interfaces are set to be very small (L/1000), while the membrane has a size of L and the electrolytes both 4L.

To capture effects caused by the electric double layer at the interface of the electrolyte and ion exchange membrane, the mesh is refined at these boundaries. Since the double layer is at the nanometer scale, the mesh should locally have a size of about 0.1 nm. To achieve this, four extra domains are defined at the electrolyte-membrane boundaries: two in the ion exchange membrane and two in the electrolytes. In these domains, the mesh size is set to be extremely small to accurately

capture double layer effects.
The mesh is set to be different for the seven domains, depending on the expected steepness of potential and concentration gradients. For the first and last domain and the membrane, the concentration gradients are not steep, so the mesh can be relatively coarse. The number of elements is set to be 80 with an element ratio of 10. For the first domain, this element ratio is set in reverse direction, making the elements finer near the membrane where gradients are steeper. For the membrane, a symmetric element ratio is applied so that the mesh is finer at its edges.
For the boundary electrolytes and the electrolyte-membrane interfaces, where double layer effects are significant, the number of elements is set to be 40 with an element ratio of 1000, resulting in an element size of about 0.1 nm at the boundaries. This is sufficiently small to capture the steep gradients associated with the double layer. Because the domains at the electrolyte-membrane interfaces are so small, their elements will be much finer than those in the electrolyte and membrane. The largest element in the system has a size of $5\mu m$, while the smallest element is 0.1nm.
In total, the domain consists of four boundary domains with 40 elements each and three coarser domains with 80 elements each, resulting in 400 elements overall. This mesh resolution has been shown to be sufficient based on the Richardson extrapolation analysis.

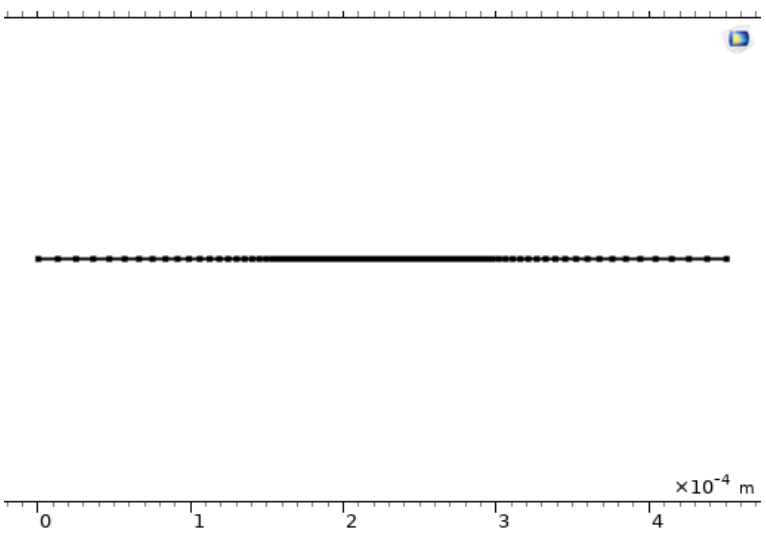

Figure 11: The mesh as shown in COMSOL. The mesh elements are larger at the bulk of the electrolyte where the concentration gradients are less steep.

Formulation of the weak form

The FEM approximates the function of interest, u, by use of linear combinations of basis functions (Detailed Explanation of the Finite Element Method (FEM), n.d.-b).

$$u \approx u_h \tag{40}$$

$$u_h = \sum_i u_i \psi_i \tag{41}$$

Where ψ_i are the basis functions and u_i are the coefficients that approximate u. In figure 12 an example of an approximation by a linear combination of basis functions is shown. Finer elements are used at places with a steeper gradient to improve accuracy. In this example linear basis functions are used, while COMSOL uses quadratic basis functions (Detailed explanation of the Finite Element Method (FEM). (n.d.-b)). Quadratic basis functions are more accurate than linear basis functions and are necessary to capture nonlinear gradients.

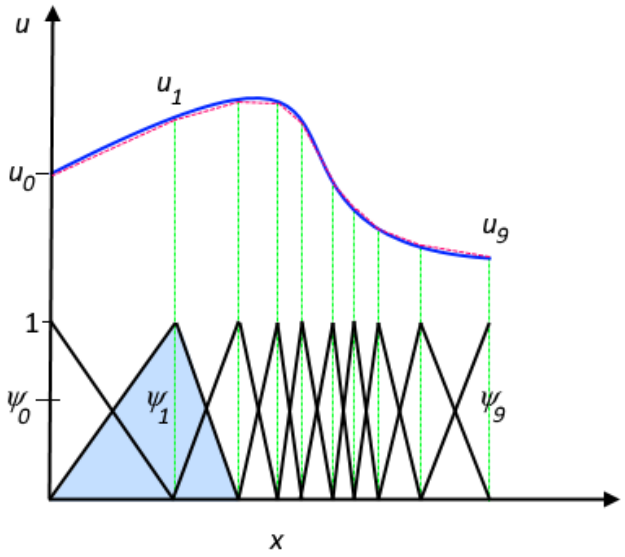

Figure 12: An example of an approximation by a linear combination of linear basis functions. The solution is approximated by a sum of basis functions ψ_i weighted by their coefficients u_i. Every basis function i is zero on the whole domain except at the ith mesh element. At steeper gradients smaller mesh elements are chosen. In the actual model quadratic basis functions are chosen for higher accuracy. (Detailed Explanation of the Finite Element Method (FEM), 2016)

For the Nernst-Planck equation for species i:

$$\frac{\partial c_i}{\partial t} + \nabla \cdot \mathbf{J}_i + \mathbf{u} \cdot \nabla c_i = R_i \tag{42}$$

Where $\mathbf{J}_i = -D_i \nabla c_i - z_i u_m F c_i \nabla \phi$.

Both sides are multiplied by a test function ψ and integrated over the domain Ω:

$$\int_\Omega \left(\frac{\partial c_i}{\partial t} + \nabla \cdot \mathbf{J}_i + \mathbf{u} \cdot \nabla c_i - R_i \right) \psi \, d\Omega = 0 \tag{43}$$

The PDE's that COMSOL solves are the Nernst-Planck equation for the three species A, B and C and the Poisson equation:

$$\frac{\partial c_i}{\partial t} + \nabla \cdot \mathbf{J}_i + \mathbf{u} \cdot \nabla c_i = R_i \tag{44}$$

Where $\mathbf{J}_i = -D_i \nabla c_i - z_i u_m F c_i \nabla \phi$.

$$-\frac{d}{dx}\left(\epsilon \frac{d\phi}{dx}\right) = F \sum_{i=A,B,C} z_i c_i \tag{45}$$

With the Dirichlet boundary conditions:

$$c_A(0) = c_B(0) = C_{Bulk}, c_C(0) = 0 \tag{46}$$

$$c_A(L_{tot}) = c_C(L_{tot}) = C_{Bulk}, c_B(L_{tot}) = 0 \tag{47}$$

And initial condition:

$$c_A = c_B = c_C = C_{Bulk} \tag{48}$$

The weak form of these PDE's is then obtained by multiplying the equations with a test function and integrating by parts. Let ψ_A, ψ_B, ψ_C be test functions for species A, B, C respectively.

$$\int_0^{L_{\text{tot}}} \frac{\partial c_i}{\partial t} \psi_i \, dx + \int_0^{L_{\text{tot}}} \frac{\partial J_i}{\partial x} \psi_i \, dx = \int_0^{L_{\text{tot}}} R_i \, \psi_i \, dx \tag{49}$$

With i = A, B, C. In order to get rid of the flux term $\frac{\partial J_i}{\partial x}$ we integrate by parts.

$$\int_0^{L_{\text{tot}}} \frac{\partial c_i}{\partial t} \psi_i \, dx - \int_0^{L_{\text{tot}}} J_i \frac{\partial \psi_i}{\partial x} \, dx + [J_i \psi_i]_0^{L_{\text{tot}}} = \int_0^{L_{\text{tot}}} R_i \, \psi_i \, dx \tag{50}$$

The weak form of the Poisson equation is then as follows:

$$\int_0^{L_{\text{tot}}} \epsilon \frac{d\phi}{dx} \frac{d\psi_\phi}{dx} \, dx = \int_0^{L_{\text{tot}}} \left(\sum_{i=A,B,C} z_i F c_i \right) \psi_\phi \, dx \tag{51}$$

Now for each variable, the solution can be approximated by using equation 52:

$$c_A(x,t) \approx \sum_j C_{A,j}(t)\,\phi_j(x) \tag{52}$$

Where $\phi_j(x)$ is the basis function corresponding to the j-th element and $C_{A,j}(t)$ is the time-dependent coefficient for the j-th basis function. COMSOL uses the Galerkin method, which means that the basis functions are the same as the test functions. Therefore the basis and test functions are quadratic (second order Lagrange polynomials).

Tolerance

For the solver, both relative and absolute tolerances are defined. The relative tolerance is set to be 0.001, which means that the relative error for each time step is limited to 0.1 percent of the solution magnitude. The absolute tolerance is set with a scaled method with a tolerance factor of 0.1. This means that the absolute tolerance for each variable is scaled based on the typical magnitude of that variable. The tolerance factor of 0.1 ensures that variables with small magnitudes don't get overshadowed by the relative tolerance. These relative errors can be too strict for very small magnitudes and therefore be too computationally demanding.

Impedance Measurements

Finally the impedance should be measured. In order to do this, an AC voltage perturbation is applied and the resulting current is measured. To add this voltage perturbation, a sine wave is created, which frequency can be varied. Now two electrolyte potential conditions are created. At the left boundary of the setup (x=0), the electrolyte potential is:

$$\phi_{l,bnd} = V_{applied} \cdot sin(\omega t) \tag{53}$$

Where $V_{applied}$ can be varied and is set to be 0.01 V, a value that is commonly used to measure impedance. And at the right boundary the electrolyte potential is 0. For a certain frequency, the system is solved for a certain amount of AC periods. The resulting voltage and current are then measured at the left boundary, which results in a voltage and current dataset that can be exported for further investigation.

Impedance calculation

The model cannot measure impedance directly. Therefore, an alternating current is applied and the resulting voltage is measured. From the current and voltage

signals, the impedance can then be calculated. First the signals are converted to their complex form:

$$I = I_0 e^{j\theta_I} \tag{54}$$

$$V = V_0 e^{j\theta_V} \tag{55}$$

Where V_0 and I_0 are the magnitudes of the voltage and current and θ_V and θ_I are their phases.
Now the impedance can easily be calculated by using the following expression for the impedance:

$$Z = Z_0 e^{j\phi} = Z_0(cos(\phi) + jsin(\phi)) \tag{56}$$

Where Z_0 is the ratio between the magnitudes of voltage and current, $\frac{V_0}{I_0}$ and ϕ is the phase difference between the current and voltage. This means that we get one measurement for every frequency, with real and imaginary parts, because the phase difference will remain constant.
To measure the impedance of the system, first the voltage and the resulting current are measured for a certain frequency. Now to determine the (complex) impedance, a Fast Fourier Transform (FFT) is performed on the data, which yields the magnitude and phase of the current and voltage. The FFT decomposes the current and potential signals into their frequency components, so their phase can be calculated. Then the impedance is given by equation 57:

$$Z = \frac{V_0 e^{j\theta_V}}{I_0 e^{j\theta_I}} \tag{57}$$

To avoid spectral leakage, the Hanning window is used, after which the Fourier transforms of the current and voltage signals are calculated. For the applied frequency, then the phase and magnitude of the current and voltage signals can be calculated. The Python code to calculate the impedance is included in the appendix. The code processes the current and voltage signals, applies the FFT, and computes the impedance for each frequency. For every different frequency, the filename is changed to match the right data, and the frequency is changed manually.

5 Results

Impedance Spectra

First, the impedance spectrum for the default values is calculated. At the lower frequencies (0.001-1 Hz), the diffusion boundary layer will have the most effect on the impedance spectrum, while at higher frequencies (1 Hz - 10 kHz), the double layer has a larger effect (Długołęcki et al., 2010). Therefore, the impedance for approximately 10 frequencies between 0.001 Hz and 1000 Hz will be calculated to form an impedance spectrum. For the different frequencies, the ion concentration profiles will also be calculated to form an idea on the behavior of the ions and their effect on the impedance.

Default Parameters

Parameter	**Value**
Size L	50 μm
Concentration c_A	0.01 M
Concentration c_B	0.01 M
Concentration c_C	0.01 M
Immobilized Ion Concentration c_{lm}	0.1 M
Applied Voltage V_{applied}	0.01 V
Temperature T	293.15 K
Diffusion Coefficients D_A, D_B, D_C	1×10^{-9} m^2/s
Electrolyte Volume Fraction ϵ_l	0.5
Relative Permittivity Membrane ϵ_r	20
Relative Permittivity Electrolyte ϵ_r	50
Membrane Area A	1×10^{-4} m^2

Table 5: Default Parameters

The uncertainty in the impedance calculation lies, in part, in the resolution of the measured voltage and current and the number of used periods. In other words, small time steps and many periods lead to more accurate impedance values. Too small time steps and too many periods, however, significantly increase computation times. From Richardson extrapolation, a mesh consisting of 400 elements is chosen. The Richardson extrapolation was applied for a 1 Hz potential from which a time step

of 0.01 s was chosen. Even though no analysis has been made for other frequencies, the same time step to period ratio of 100 will be used because further refinements at different frequencies have not led to significantly different results.
The impedance spectrum for the default values is shown in figure 13:

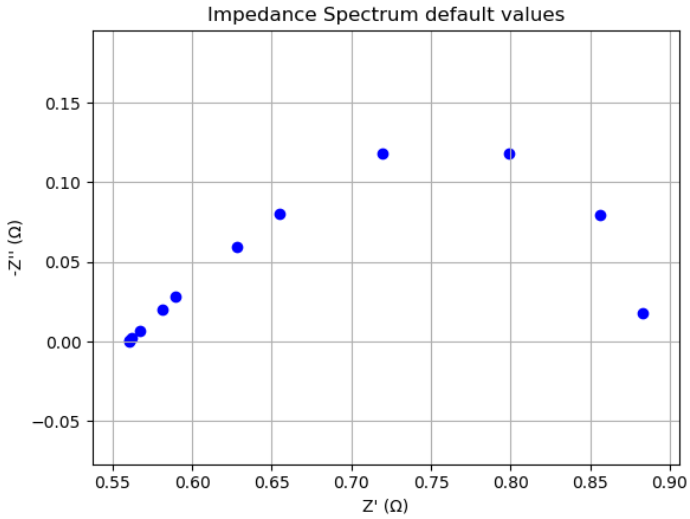

Figure 13: Impedance spectrum for the default values.

Here the points on the left denote higher frequencies, and on the right lower frequencies.

Concentration Profiles

To explain the shape of the impedance spectrum, the corresponding ion concentration profiles are investigated. For example, the ion concentration profiles for 0.001, 0.02, 1, and 100 Hz are shown:

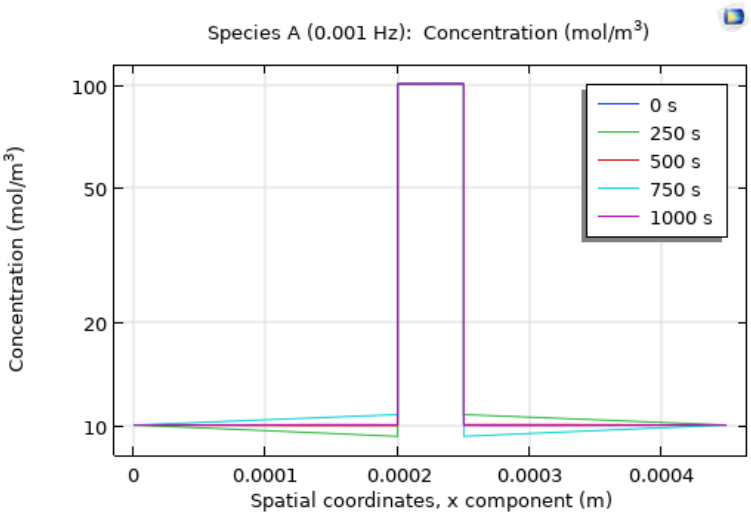

Figure 14: Concentration profile of species A at 0.001 Hz. One period of the signal is shown, and the y-axis is taken to be on a logarithmic scale to distinguish the change in concentration.

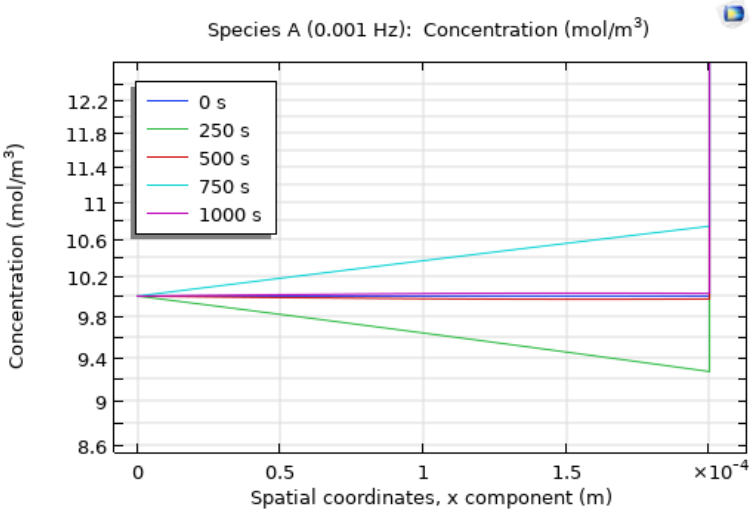

Figure 15: The diffusion boundary layer of species A at 0.001 Hz. The concentration starts at $10 mol/m^3$ and then moves down and up again.

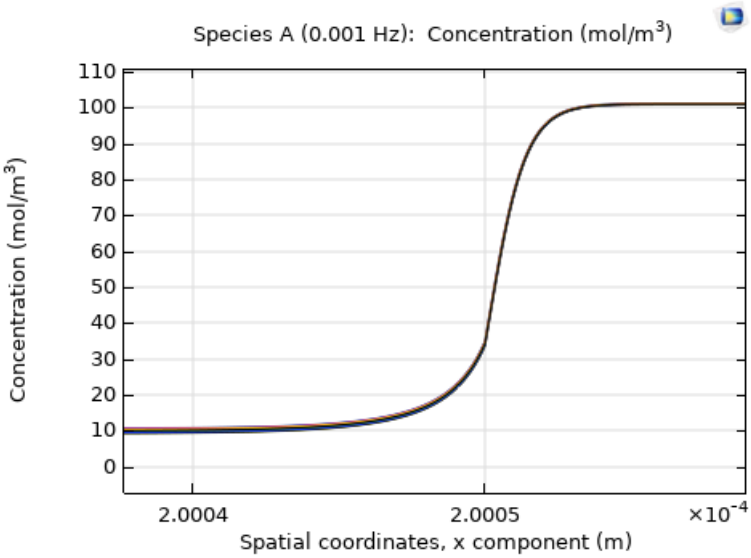

Figure 16: The electric double layer of species A at 0.001 Hz. The double layer is relatively stable.

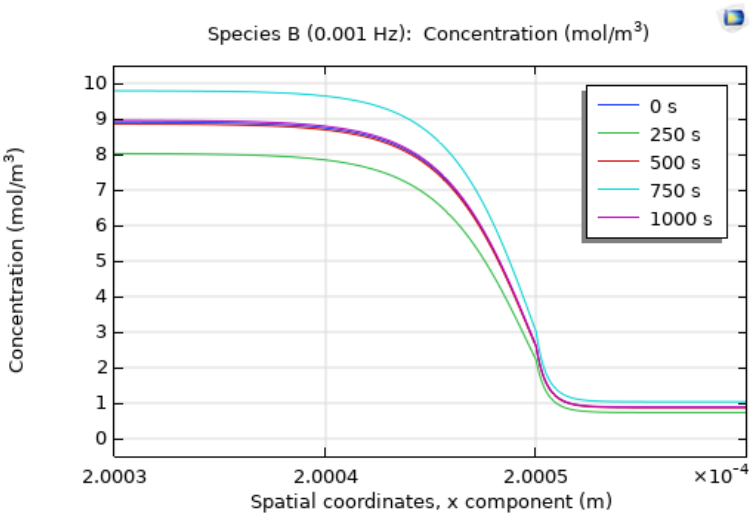

Figure 17: The electric double layer of species B at 0.001 Hz. This double layer oscillates between concentrations of 8 and 10 mol/m^3

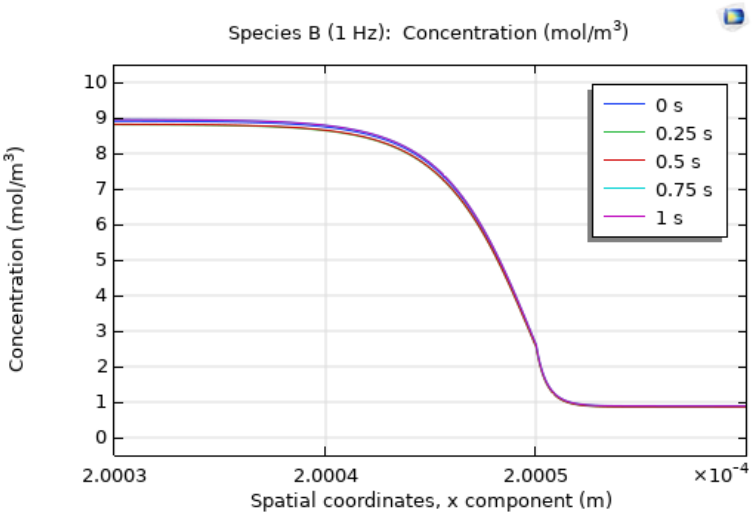

Figure 18: The electric double layer of species B at 1 Hz. The double layer is more stable and the difference in concentration is difficult to distinguish.

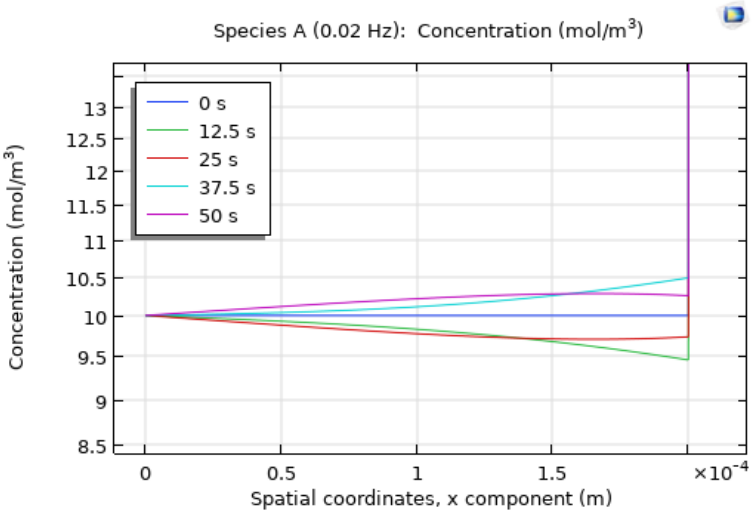

Figure 19: The diffusion boundary layer of species A at 0.02 Hz.

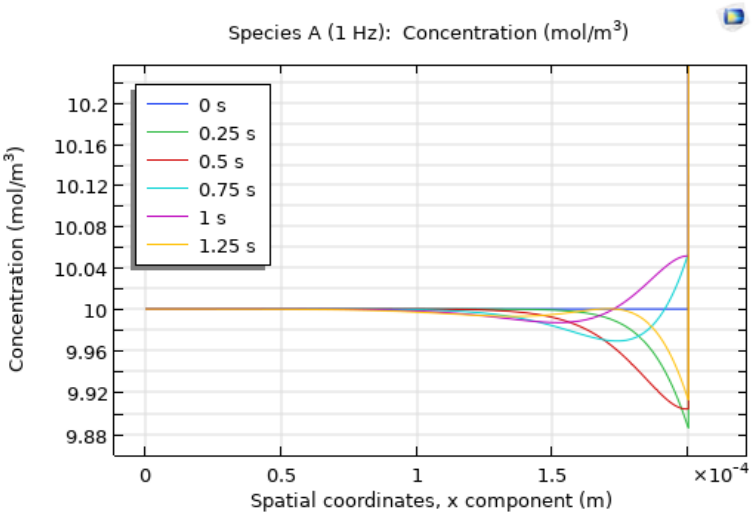

Figure 20: The diffusion boundary layer of species A at 1 Hz.

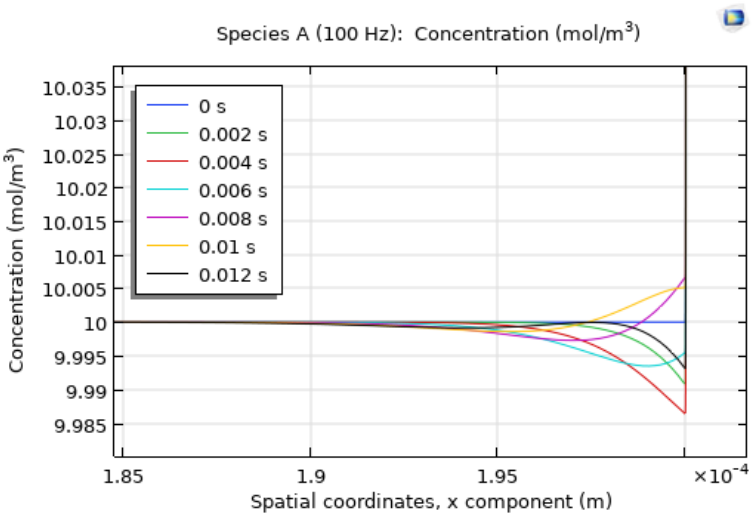

Figure 21: The diffusion boundary layer of species A at 100 Hz.

Because the double layer for the cation is almost identical for different frequencies, only the figure for 0.001 Hz is included. The relative difference between different double layers for species B is much larger as seen in the figures. However, the diffusion boundary layer shows much more variance for different frequencies. Therefore, the shape of the impedance spectrum is mainly caused by the diffusion boundary layer. At larger frequencies the diffusion boundary layer does not have enough time to form, which causes the impedance to be mostly real. At low frequencies the ions have enough time to move to a linear concentration profile, while at higher

frequencies the concentration gradients get steeper and the diffusion boundary layer gets smaller. The capacitance is maximal around 0.02 Hz and decreases for higher and lower frequencies. The resistance decreases for higher frequencies because the diffusion layer has less time to form, as shown in the figures.

Concentration

Now the impedance spectrum for different ion concentrations will be determined.

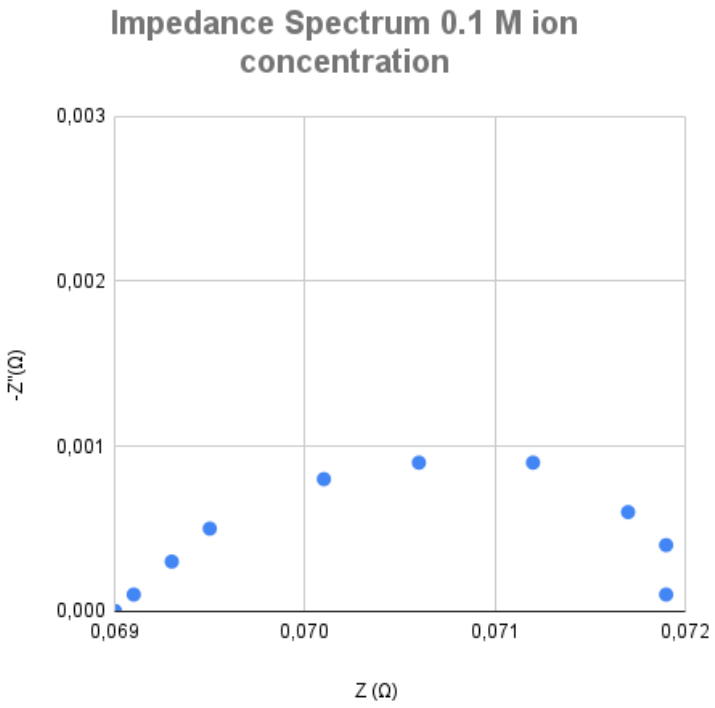

Figure 22: The impedance spectrum for species concentrations $C_A, C_B, C_C of 0.1M$.

The double layer for 100 Hz is shown in figure 23:

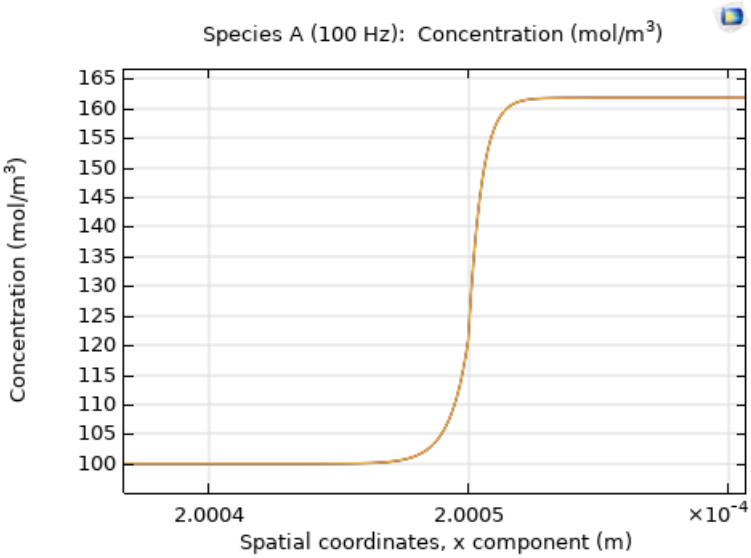

Figure 23: The double layer of species A for 100 Hz and species concentration of 0.1 M.

Compared to an ion concentration of 0.01 M, the double layer is more compressed. Just as for the default values, the double layer is similar for different frequencies. The diffusion boundary layer for various frequencies is shown in the following figures.

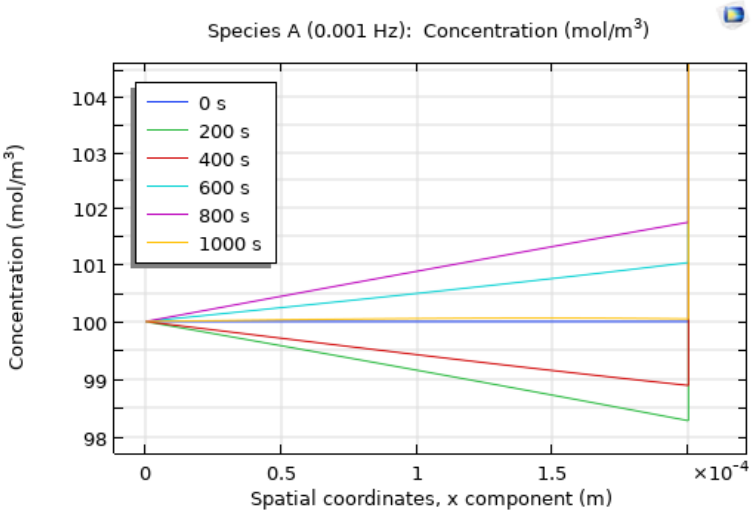

Figure 24: The diffusion boundary layer for species A at 0.001 Hz and species concentration of 0.1 M.

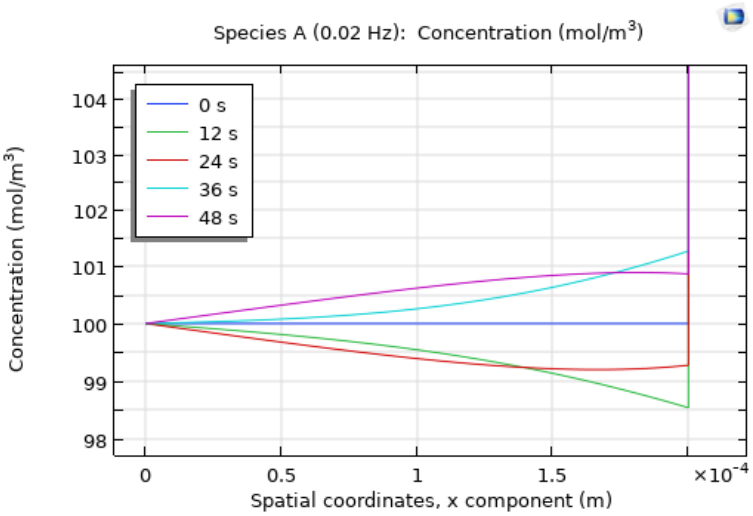

Figure 25: The diffusion boundary layer of species A at 0.02 Hz and a species concentration of 0.1 M.

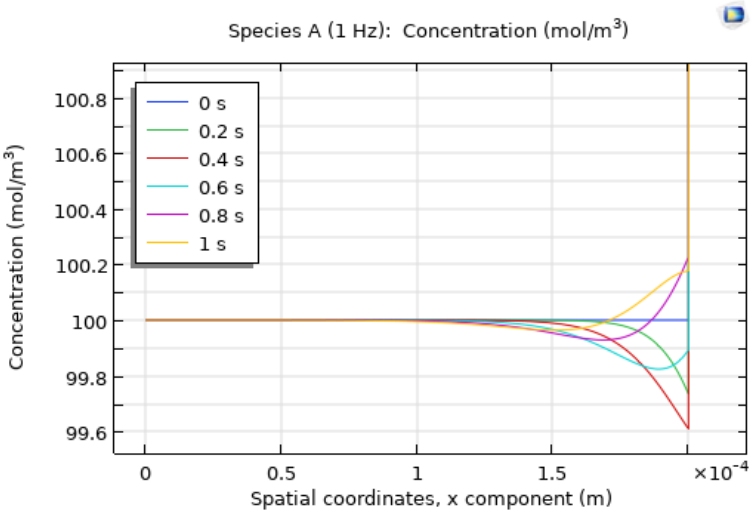

Figure 26: The diffusion boundary layer of species A at 1 Hz and a species concentration of 0.1 M.

Again, at the lower frequencies, larger boundary layers can form. Because the double layer is similar for different frequencies, the diffusion layer has the largest influence on the impedance spectrum. Compared to an ion concentration of 0.01 M, the impedance is about ten times smaller.
In figure 27 the impedance spectrum for an ion concentration of 0.002 M is shown.

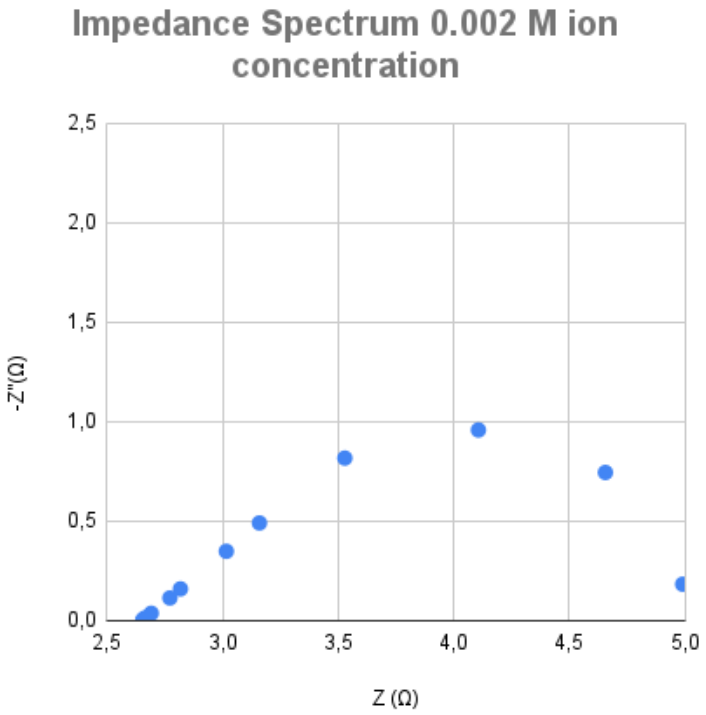

Figure 27: The impedance spectrum for species concentrations $C_A, C_B, C_C of 0.002 M$.

Both the real and imaginary impedance are much larger for the lower ion concentration.

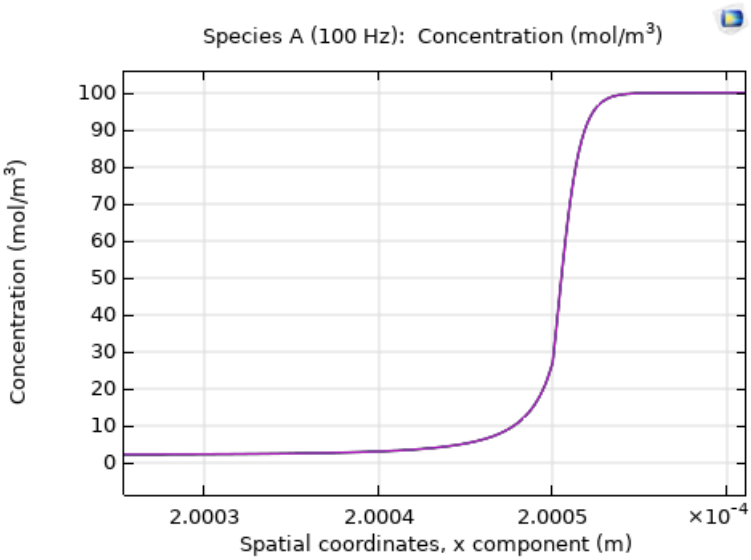

Figure 28: The double layer of species A for 100 Hz and species concentration of 0.002 M.

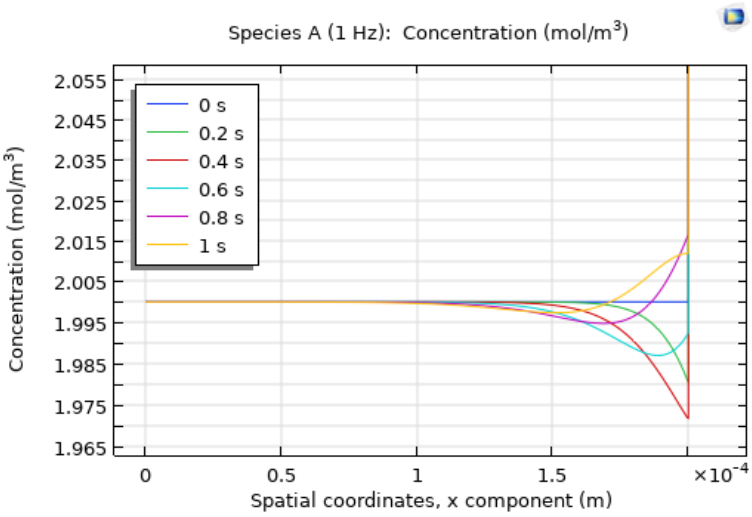

Figure 29: The diffusion boundary layer of species A at 1 Hz and a species concentration of 0.002 M.

Fixed Membrane Charge

Now the influence of the fixed space charge in the membrane on the impedance spectrum is investigated. For fixed ion concentrations of 0.2 M and 0.02 M (0.1 M is the default), the impedance spectra are determined, and the double layer and diffusion layer are shown for identical frequencies. A larger fixed space charge caused a rise of ion concentration in the membrane to counter the fixed charge. This means that the double layer will also be larger, but the shape remains the same. Because the concentration of the ions in the membrane is higher, the diffusion boundary layer will also have higher concentration gradients. However, the length of the diffusion layer stays the same. The main difference in the impedance spectrum is an increase in reactance for larger fixed space charges and an increase in resistance. This is caused by the increased diffusion impedance caused by higher concentration gradients.

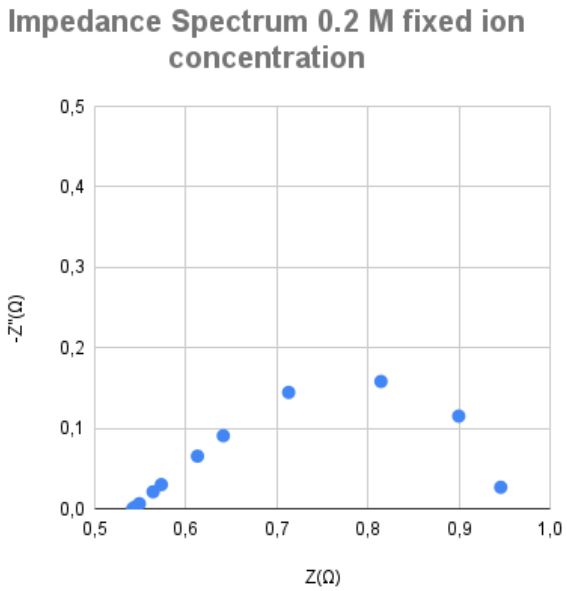

Figure 30: The impedance spectrum for a fixed ion concentration of 0.2 M.

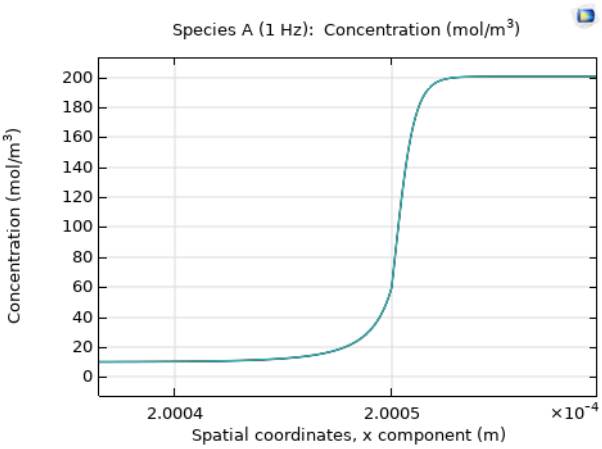

Figure 31: The double layer of species A for 1 Hz and fixed ion concentration of 0.2 M.

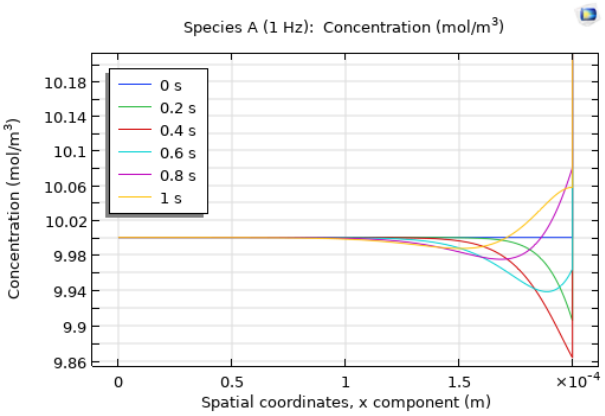

Figure 32: The diffusion boundary layer of species A at 1 Hz and a fixed ion concentration of 0.2 M.

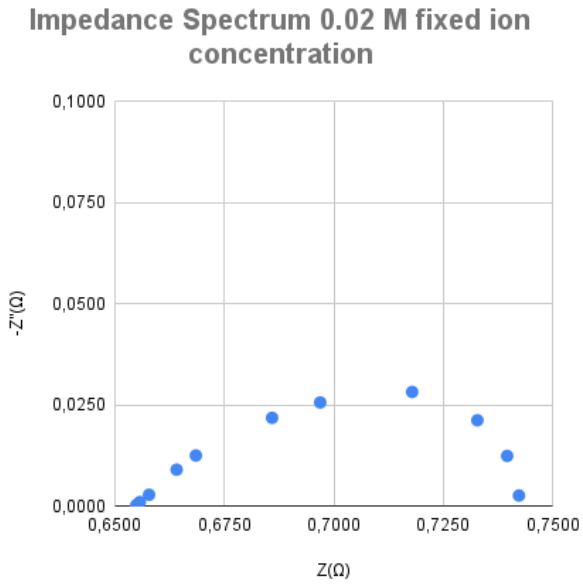

Figure 33: The impedance spectrum for a fixed ion concentration of 0.02 M.

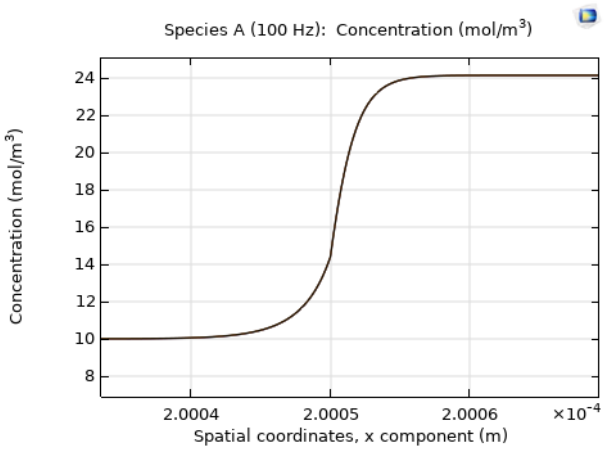

Figure 34: The double layer of species A for 100 Hz and fixed ion concentration of 0.02 M.

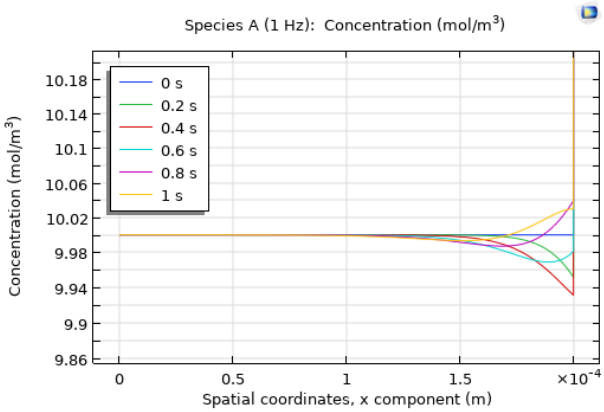

Figure 35: The diffusion boundary layer of species A at 1 Hz and a fixed ion concentration of 0.02 M.

Diffusion Coefficients

Now the diffusion coefficients will be investigated. First, the diffusion coefficient of species A is varied. The diffusion coefficient typically ranges from $10^{-10}m^2/s$ to $10^{-9}m^2/s$ but for now the impedance spectrum for a diffusion coefficient of $10^{-10}m^2/s$ and of $10^{-8}m^2/s$ will be obtained.

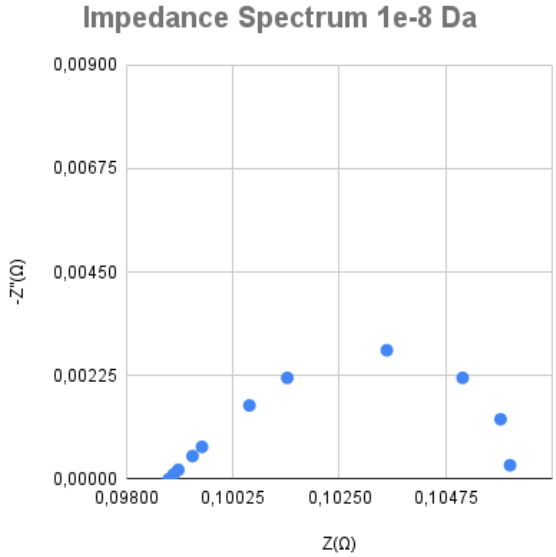

Figure 36: The impedance spectrum for the diffusion coefficient of species A of $1e-8m^2/s$.

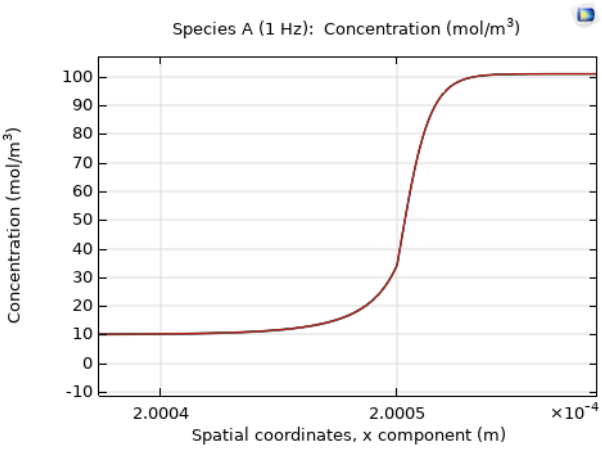

Figure 37: The double layer for species A at 1 Hz for the diffusion coefficient of species A of $1e-8m^2/s$.

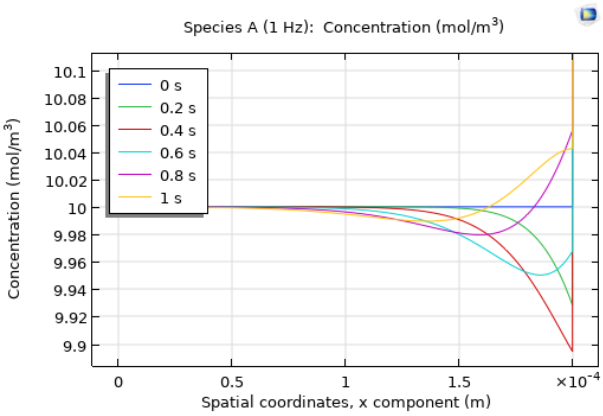

Figure 38: The diffusion boundary layer at 1 Hz for the diffusion coefficient of species A of $1e-8 m^2/s$.

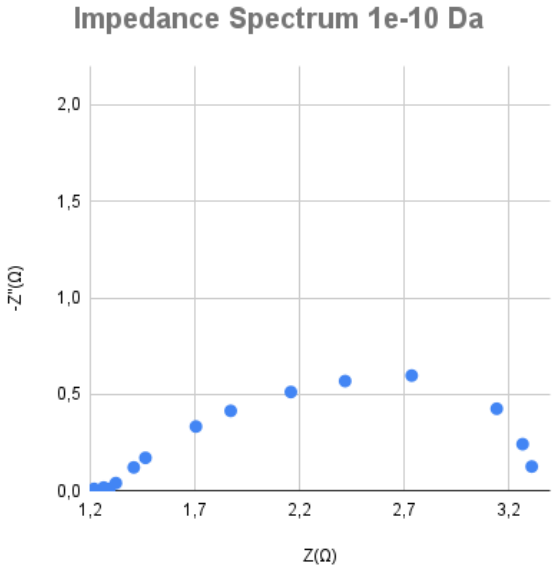

Figure 39: The impedance spectrum for the diffusion coefficient of species A of $1e-10 m^2/s$.

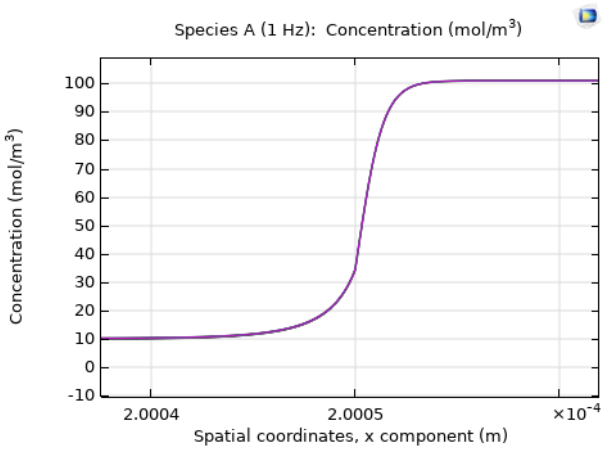

Figure 40: The double layer at 1 Hz for the diffusion coefficient of species A of $1e-10m^2/s$.

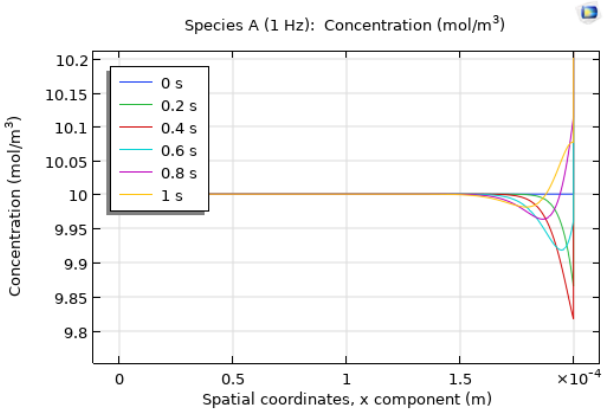

Figure 41: The diffusion boundary layer at 1 Hz for the diffusion coefficient of species A of $1e-10m^2/s$.

Now the diffusion coefficients of species B and C will also be varied. The impedance spectrum for diffusion coefficients D_a, D_B, D_c equal to $10^{-8}m^2/s$ is shown in figure 42:

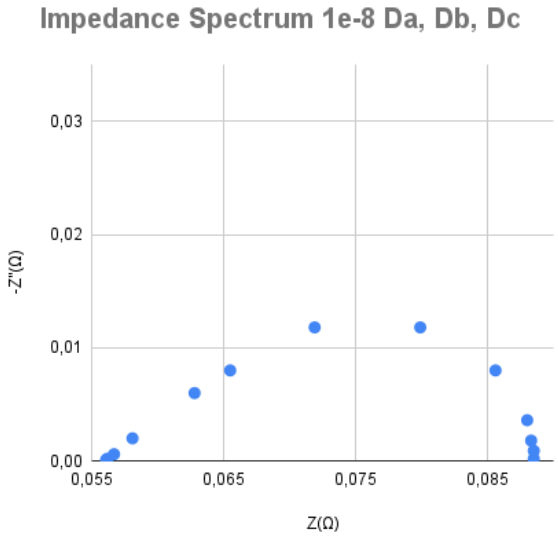

Figure 42: The impedance spectrum for the diffusion coefficient of species A, B, C of $1e-8m^2/s$.

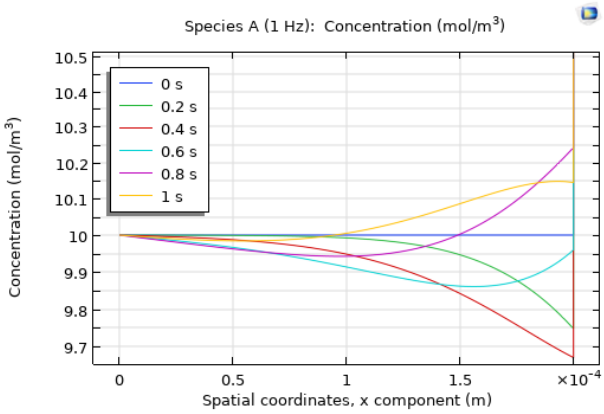

Figure 43: The diffusion boundary layer at 1 Hz for the diffusion coefficient of species A, B, C of $1e-8m^2/s$.

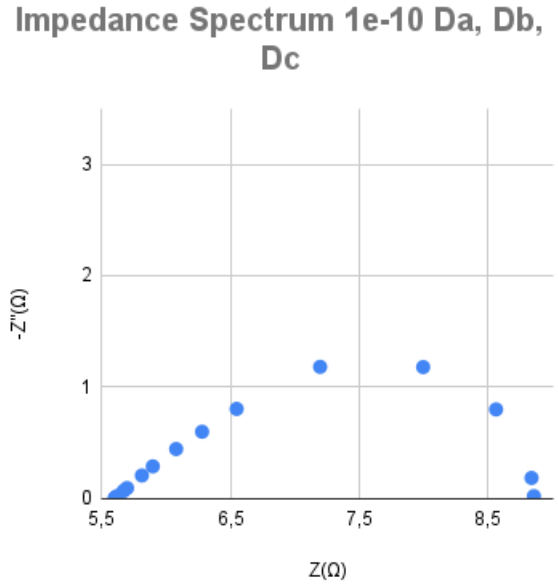

Figure 44: The impedance spectrum for the diffusion coefficient of species A, B, C of $1e-10m^2/s$.

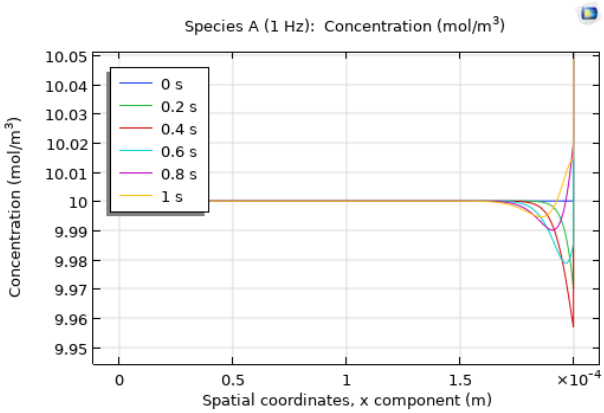

Figure 45: The diffusion boundary layer for the diffusion coefficient of species A, B, C of $1e-10m^2/s$.

When only D_a is increased by a factor 10, the imaginary impedance decreases by a factor of 40, while the real impedance decreases with a factor of about 5 to 10. When D_a is decreased by a factor 10 the imaginary impedance increases by a factor 5 while the real impedance increases by a factor of about 3. The double layer does not change, but the diffusion boundary layer grows for a larger diffusion coefficient and gets compressed for a smaller diffusion coefficient. This can be explained by equation 19, larger diffusion coefficients will lead to an increase in the flux. This

means a higher current for the same potential, so a decrease in impedance. An increased mobility will also mean that the diffusion layer needs less time to build up, so it will be larger for higher diffusion coefficients.

Relative Permittivity

Relative membrane permittivity ranges from 5-80. For a relative permittivity of 5 instead of 20, the impedance values are all slightly lower; for a relative permittivity of 80 instead of 20, the impedance is slightly higher. The impedance spectra for different relative permittivities are plotted in figure 46:

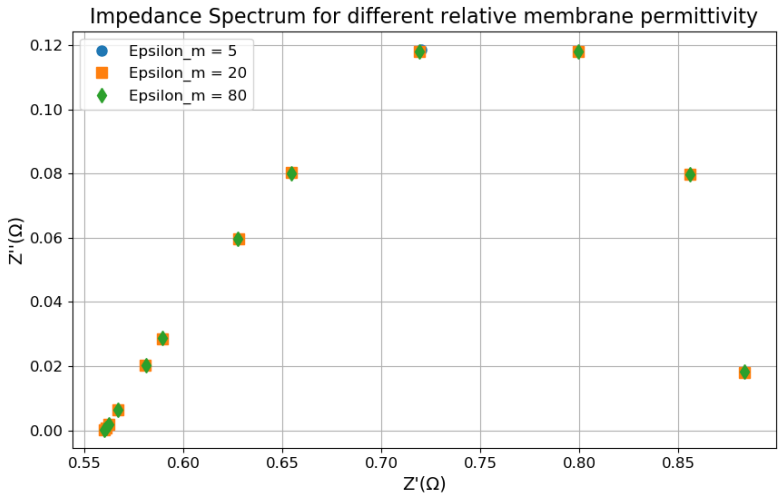

Figure 46: The impedance spectrum for relative membrane permittivities of 5, 20, and 80.

It is clear from the figure that the relative permittivity of the membrane has little to no influence on the impedance spectrum. For the different permittivities, however, there is a difference in the double layer:

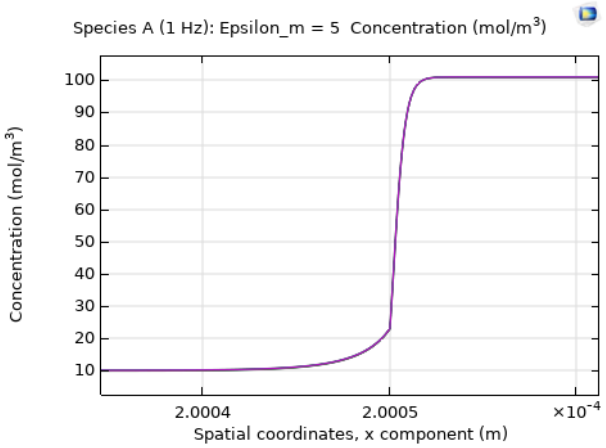

Figure 47: The double layer for a relative membrane permittivity of 5.

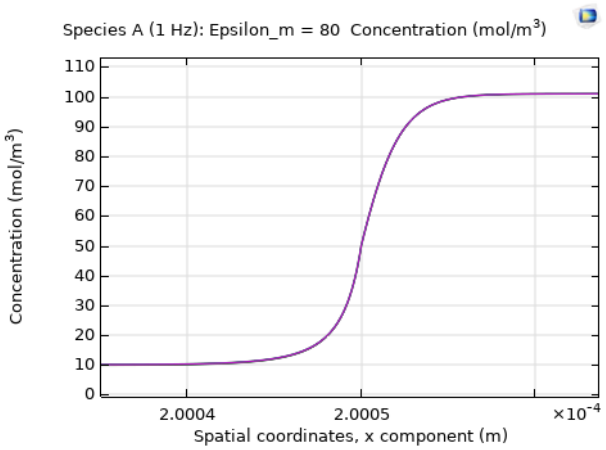

Figure 48: The double layer for a relative membrane permittivity of 80.

For a larger relative permittivity, the double layer will be more pronounced. The earlier observation that in this setup the double layer has little effect on the impedance spectrum is therefore confirmed since a change in the double layer has little to no effect on the impedance. By equation 23 the relative permittivity determines how much electric energy the material can store. Therefore, higher permittivities should lead to larger double layers, which is shown in the figures.
Relative electrolyte permittivities usually range between 10 and 80. However, similar to the membrane relative permittivity, the electrolyte permittivity has very little effect on the impedance and therefore is not investigated further.

Electrolyte Volume Fraction

The electrolyte volume fraction has no influence on the diffusion boundary layer and the double layer, but it does lower the membrane resistance. The impedance spectra for different volume fractions are shown in figure 49:

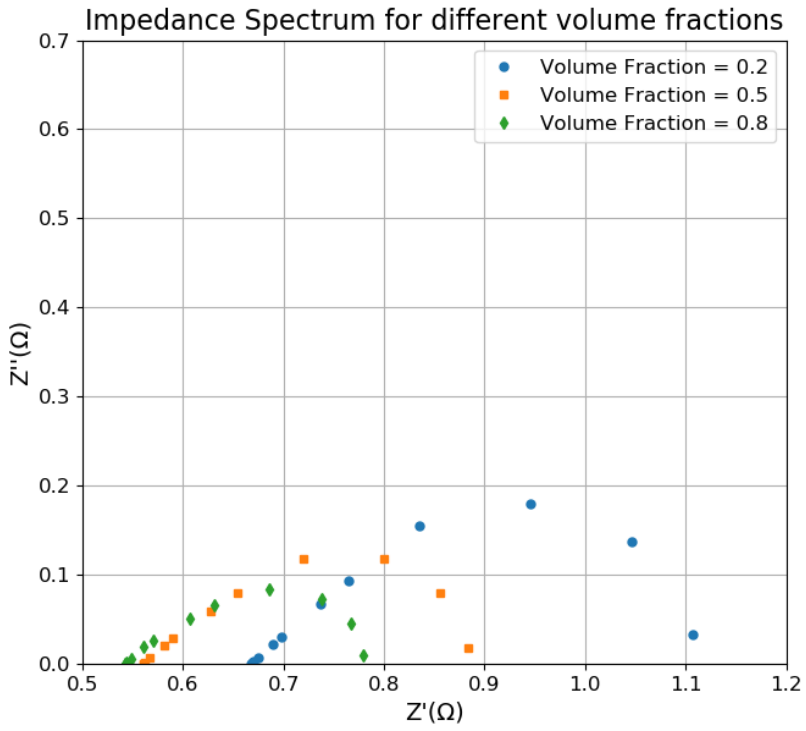

Figure 49: The impedance spectrum for an electrolyte volume fraction in the membrane of 0.2, 0.5, and 0.8.

The figure shows a decrease in resistance and reactance for increasing volume fraction while the shape of the spectrum remains the same.
The results are consistent with earlier research. The impedance spectra are similar in shape, but the impedance is a lot lower in the used COMSOL model. This is mainly because of the very large surface area used in the model.

Equivalent Circuit

Now the impedance spectrum will be fitted to the different equivalent circuits described in the literature review. First, the equivalent circuit is assumed to contain two capacitors representing the electric double layer and diffusion boundary layer. For the second fit, the diffusion layer is assumed to be a constant phase element,

and for the last fit, both the double layer and the diffusion layer are assumed to be constant phase elements. For this example, the default parameter values are used except for the membrane surface, which is reduced to $1e-4m^2$ to approach more realistic impedance values.

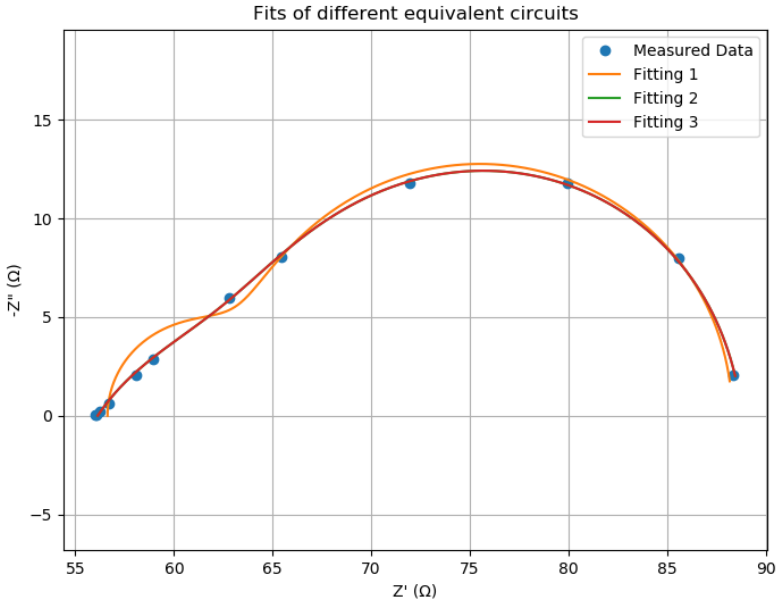

Figure 50: In the figure the different equivalent circuits are fitted to the measured data. Fit 2 and 3 are identical, which means that one of the components can be approached as an ideal capacitor.

The corresponding parameters are shown in the tables.

Table 6: Optimized Parameters for Model 1

Parameter	**Value**
R0	56.63018358
R1	6.83660396
C1	0.08136505
R2	24.83754462
C2	0.44828316

Table 7: Optimized Parameters for Model 2

Parameter	**Value**
R0	56.12655154
R1	21.19423887
C1	0.55908604
R2	11.58855458
Q2	0.10077253
α_2	0.62309403

Table 8: Optimized Parameters for Model 3

Parameter	**Value**
R0	56.12655307
R1	21.19429389
C1	0.55908453
α_1	1.0
R2	11.58848405
Q2	0.10077218
α_2	0.623096

Because the capacitive elements corresponding to the double layer and diffusion boundary layer are placed in series, their impedance contributions are interchangeable. Therefore, it is not possible to determine which component can be approached as an ideal capacitor from the fits.

6 Conclusion

The results show that the impedance characteristics are influenced by many different factors like the ion concentration, diffusion coefficient, and membrane properties.

For this particular setup, the impedance spectrum is mainly formed by low frequencies at which the diffusion boundary layer has the largest contribution. At higher frequencies the diffusion boundary layer has not enough time to form, which causes the impedance to decrease, while at very low frequencies the diffusion boundary layer will reach steady state, which causes the imaginary impedance to decrease.

Increases in resistance are caused by a decrease in concentration, a decrease in diffusion coefficients, or a decrease in the electrolyte volume fraction in the membrane. Causes for an increase in reactance are a decrease in the concentration, electrolyte volume fraction, or diffusion coefficient, and an increase in the fixed space charge of the membrane. For smaller membrane surface areas, the impedance will also increase.

Higher ion concentrations cause higher ionic conductivity, which causes a decrease in overall resistance and lower concentration gradients, which also causes the reactance to decrease. Higher diffusion coefficients will also cause a decrease in the impedance because of increased ion mobility and lower concentration gradients in the diffusion boundary layer. The fixed space charge in the membrane mainly affects the capacitive properties of the setup. A larger fixed space charge both causes larger concentration profiles and a larger double layer. A larger membrane relative permittivity does not have a significant effect on the impedance, while it does affect the double layer. This fact in combination with the dominance of low frequencies in the impedance spectrum suggests that the diffusion boundary plays a major role in the impedance of this system. The electrolyte volume fraction in the membrane has a large effect on the membrane resistance. For a larger volume fraction, the ion mobility in the membrane increases, which also lowers the diffusion impedance.

Because of the limited influence of the double layer, the impedance spectrum is mainly shaped by the diffusion boundary layer, which can therefore be represented by a constant phase element. The exact parameters that determine this constant phase element could be investigated further.

Richardson extrapolation has shown that the numerical accuracy in the impedance calculations is sufficient. For a mesh consisting of 400 elements, the numerical results were close to the extrapolated results, with convergence order p exceeding 2 in all

cases. The extrapolation confirmed that a time step of 0.01 s is sufficient to ensure stability and accuracy, minimizing computational cost without sacrificing precision. These validations highlight the robustness of the modeling approach and confirm the reliability of the results across multiple parameter ranges.

This study gives an insight into the parameters that can shape the impedance and the involved ion transport, providing important insights for the optimization of electrochemical systems. Future research could investigate different parameters or more complex models.

7 Recommendations

In the model in COMSOL, no existing materials are used, but instead the properties of the ions and membrane are determined and varied. A more realistic approach could be to use predefined materials and their properties. The membrane surface area of 0.01 m^2 is also quite large for an ion exchange membrane. This causes the impedance values to be lower than most experimentally observed values. In further research this parameter could also be varied to better investigate the effect of the surface area on the impedance.

Although the impedance calculation already is very accurate, the resolution of the voltage and current signals could still be improved. More importantly, Richardson extrapolation was only used at 1 Hz. Potential inaccuracies at different frequencies might have been overlooked. Richardson extrapolation could also be implemented for different membrane and ion properties for more accuracy.

The obtained impedance of the model can also be compared to experimentally obtained data with similar membranes to validate the model in COMSOL.

Although the equivalent circuit with parameters shown in table 8 already fits well to the data, alternative equivalent circuits could be fitted to capture different or more complex model behavior.

Instead of only three, multiple ion species could be used to assess their impact on the impedance. Also, more parameters could be varied, such as temperature, membrane thickness, and electrolyte sizes.

In the impedance calculation in COMSOL, a 0.01 V potential was used, which is also commonly used in real systems. However, to be able to ensure linearity of the system, this amplitude could be decreased.

The exact parameters that influence the flatness of the semicircle could also be investigated further.

Furthermore, the model could be expanded to 2D or 3D to yield more realistic results.

References

Zhang, L., Zhao, H., Wilkinson, D. P., Sun, X., & Zhang, J. (2020). Electrochemical water electrolysis: Fundamentals and Technologies. CRC Press.

Kumar, S., & Himabindu, V. (2019). Hydrogen production by PEM water electrolysis – A review. Materials Science for Energy Technologies, 2(3), 442–454. https://doi.org/10.1016/j.mset.2019.03.002

Lin, J., Zhang, Y., Xu, P., & Chen, L. (2023). CO2 electrolysis: Advances and challenges in electrocatalyst engineering and reactor design. Materials Reports: Energy, 3(2), 100194. https://doi.org/10.1016/j.matre.2023.100194

Ahuja, S. M. (2014). Comprehensive water quality and purification. http://ci.nii.ac.jp/ncid/BB178

Długołęcki, P., Ogonowski, P., Metz, S., Saakes, M., Nijmeijer, K., & Weßling, M. (2010). On the resistances of membrane, diffusion boundary layer and double layer in ion exchange membrane transport. Journal of Membrane Science, 349(1–2), 369–379. https://doi.org/10.1016/j.memsci.2009.11.069

Ekström, H. (2021, February 8). How to model Ion-Exchange membranes and Donnan Potentials. COMSOL. https://www.comsol.com/blogs/how-to-model-ion-exchange-membranes-and-donnan-potentials

Zhang, W., Ma, J., Wang, P., Wang, Z., Shi, F., Liu, H. (2016). Investigations on the interfacial capacitance and the diffusion boundary layer thickness of ion exchange membrane using electrochemical impedance spectroscopy. Journal Of Membrane Science, 502, 37–47. https://doi.org/10.1016/j.memsci.2015.12.007

Bardini, L. (2020). EIS 101 An Introduction to Electrochemical Impedance Spectroscopy. https://www.researchgate.net/publication/280009629$_E IS_1 01_a n_i ntroduction_t o_e lectroche$

Vuik, C., Vermolen, F., Van Gijzen, M., & Vuik, M. (2023). Numerical methods for ordinary differential equations. In TU Delft Open eBooks. https://doi.org/10.5074/t.2023.001

COMSOL (2016), Detailed explanation of the Finite Element Method (FEM). https://www.comsol element-method

Embree, M. (2006). Lecture 26: Richardson Extrapolation. Numerical Analysis. Virginia Tech. https://personal.math.vt.edu/embree/math5466/lecture26.pdf

Zienkiewicz, O. C., Taylor, R. L. (2000). The Finite Element Method

Frei, W. (2020, January 15). Solving nonlinear static finite element Problems | COMSOL blog. COMSOL. https://www.comsol.com/blogs/solving-nonlinear-static-finite-element-problems

Sata, T. (2007). Properties, characterization and microstructure of ion exchange membranes. In Royal Society of Chemistry eBooks (pp. 89–134). https://doi.org/10.1039/9781847
00089

Python Code

Listing 1: Impedance Calculation Python Code

```
import numpy as np
import matplotlib.pyplot as plt

def calculate_impedance(filename, target_frequency):
#Load the data, skip the first few rows in the txt file
    data = np.loadtxt(filename, skiprows=9)

    time = data[:, 0]
    voltage = data[:, 1]
    current = data[:, 2]
#Take the Hanning window to avoid spectral leakage
    window = np.hanning(len(time))
    current *= window
    voltage *= window

    voltage_fft = np.fft.fft(voltage)
    current_fft = np.fft.fft(current)
    frequencies = np.fft.fftfreq(len(time), d=(time[1] - time[0]))

    fundamental_idx = np.argmin(np.abs(frequencies - target_frequency))

    voltage_fft /= len(time)
    current_fft /= len(time)

    V_magnitude = np.abs(voltage_fft[fundamental_idx])
    I_magnitude = np.abs(current_fft[fundamental_idx])
    V_phase = np.angle(voltage_fft[fundamental_idx])
    I_phase = np.angle(current_fft[fundamental_idx])

    Z_magnitude = V_magnitude / I_magnitude
    Z_phase = V_phase - I_phase
    Z_real = Z_magnitude * np.cos(Z_phase)
    Z_imag = Z_magnitude * np.sin(Z_phase)
```

```
    Z_complex = Z_real + 1j * Z_imag

    return Z_complex

#For every frequency a seperate data file is loaded from COMSOL
data_file = 'BEP_100Hz00001A.txt'
#The frequency is defined for every different data file
frequency = 100

Z = calculate_impedance(data_file, frequency)
print(f"Impedance (Z) at {frequency} Hz: {Z:.4f} ohms")
```

Listing 2: Richardson Extrapolation Python Code

```
import numpy as np
from scipy.optimize import curve_fit

# Data: mesh sizes (h) and corresponding concentrations (v)
h_values = np.array([18.182, 9.091, 4.545, 2.273, 1.136, 0.568, 0.284])
v_values = np.array([9.9599898, 9.9598695, 9.9598549, 9.9598475, 9.9598

# Richardson extrapolation model
def richardson_model(h, u, C, p):
    return u + C * h**p

# Loop through subsets of h-values
for i in range(3, len(h_values) + 1):
    h_subset = h_values[:i]
    v_subset = v_values[:i]

    # Perform curve fitting
    params, covariance = curve_fit(richardson_model, h_subset, v_subset

    # Extract the parameters
    u_opt, C_opt, p_opt = params
```